

X-Ray Magnetic Circular Dichroism of Epitaxial $\text{Co}_2\text{Cr}_{1-x}\text{Fe}_x\text{Al}$

Bruce M. Clemens*, Raj Kelekar[†] and Hendrik Ohldag^{††}

*Department Materials Science and Engineering

[†]Department of Applied Physics

Stanford University

^{††} Advanced Light Source and SSRL

Workshop on Advanced Magnetic Spectroscopy

Advanced Light Source Users' Meeting

October 10, 2006

Outline

- I. Description of Half Metals and Reasons For Studying $\text{Co}_2\text{Cr}_{1-x}\text{Fe}_x\text{Al}$
- II. Epitaxial Growth and Basic Characterization of $\text{Co}_2\text{Cr}_{1-x}\text{Fe}_x\text{Al}$
- III. Incorporation of Epitaxial $\text{Co}_2\text{Cr}_{1-x}\text{Fe}_x\text{Al}$ into Superlattices and Spin Valves
- IV. Electronic and Magnetic Properties of Single-Layer Epitaxial Films
 - A. Measurement of the Spin Polarization
 - B. Study of the Elemental Magnetic Moments
 - C. Quantifying Atomic Disorder
- VI. Conclusions

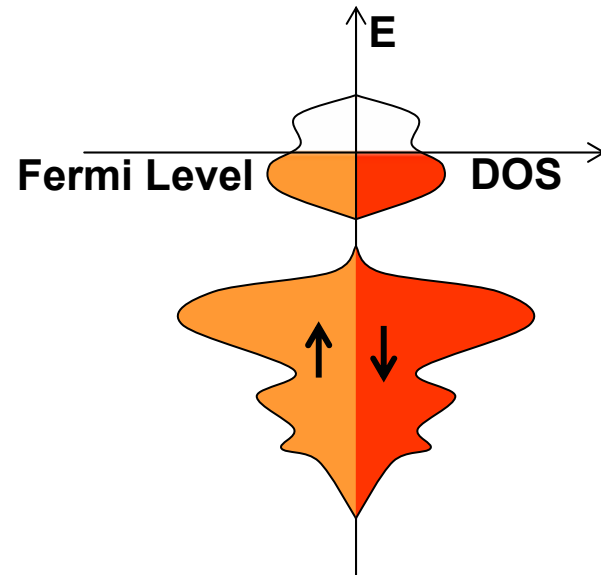
The Concept of a Half-Metal

- Ferromagnetic and metallic
- Energy gap in one spin channel at Fermi level
- First predicted in 1983 for NiMnSb deGroot et al, Phys. Rev. Lett. 50, 2024 (1983)
- All examples based upon band structure calculations

Half-Metallic Density of States

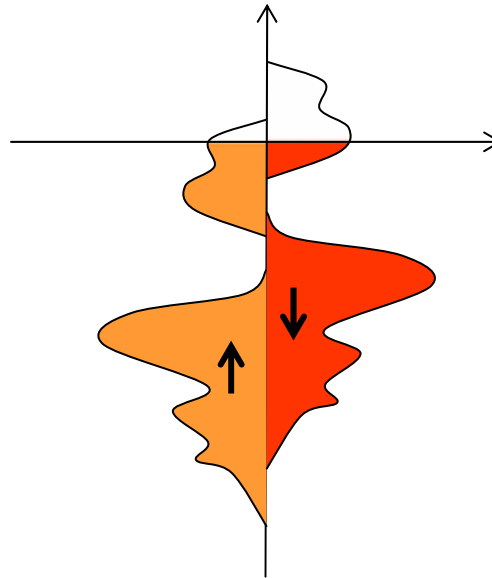
Nonmagnetic
Metal

e.g. Cu, Mg, Au



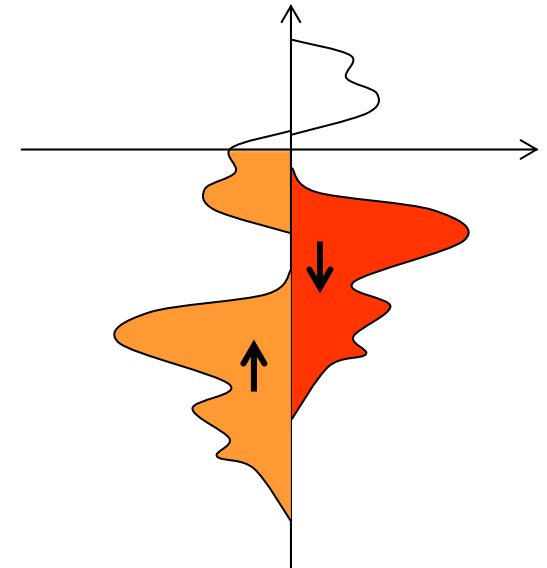
Ferromagnetic
Metal

e.g. Fe, Co, Ni



Half Metal

e.g. CrO_2



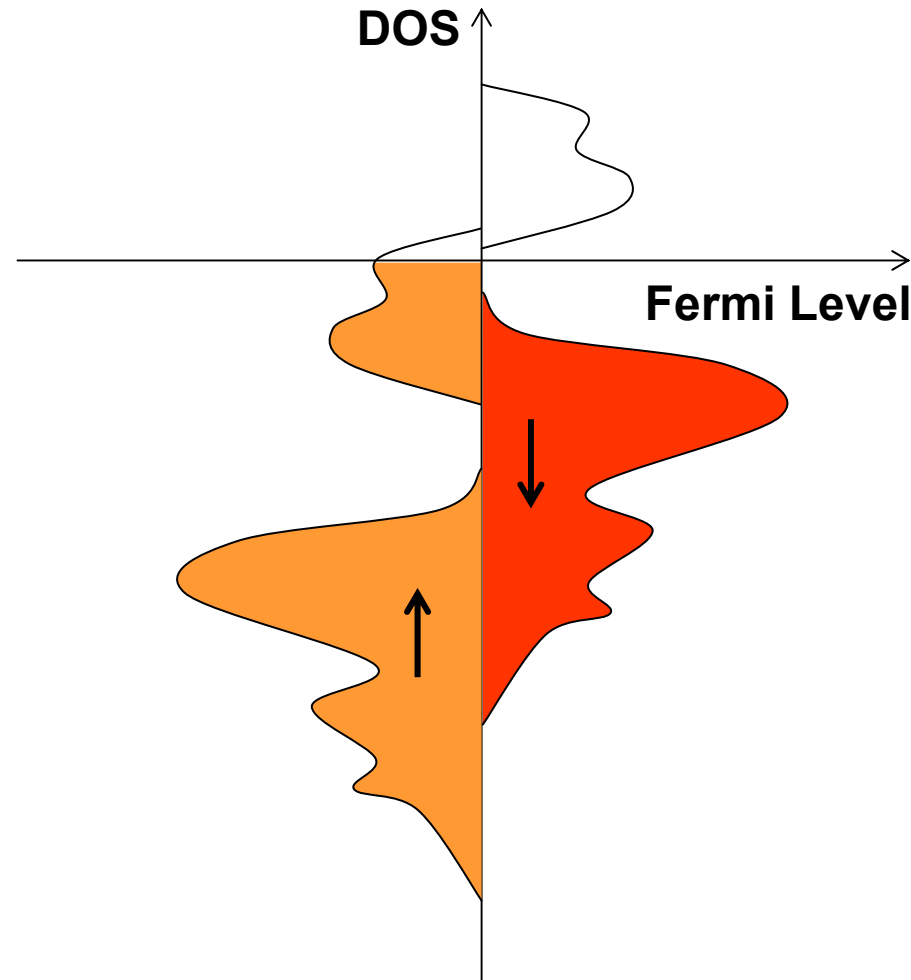
Signature of Half-Metals

- 100 % spin polarization P

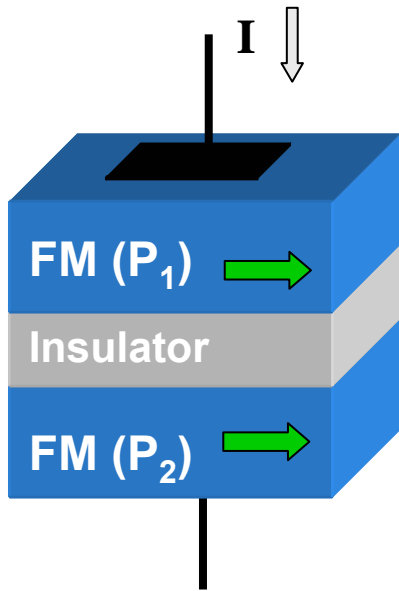
$$P = \frac{n_{\uparrow} - n_{\downarrow}}{n_{\uparrow} + n_{\downarrow}} \text{ at Fermi level}$$

- The filled spin channel has an integer number of electrons

- $M_s = Z - n$ (thumb rule)
in μB / formula unit
 Z = number of valence e-
 n = an integer



Applications: Tunneling Magnetoresistance

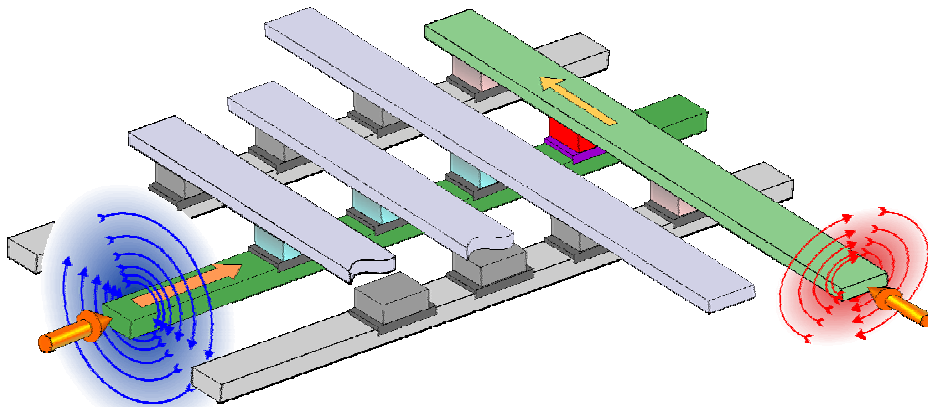
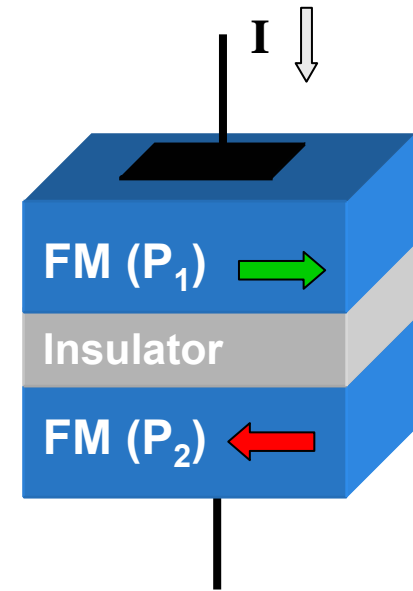


→ = direction of magnetization

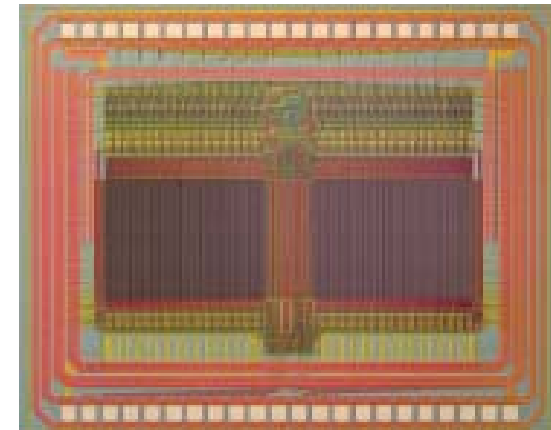
FM = Ferromagnet

$$\frac{R_{AP} - R_P}{R_P} = \frac{2P_1P_2}{1 - P_1P_2}$$

Julliere, Phys. Lett. 54A, 225 (1975)



MRAM crosspoint architecture



MRAM chip by Motorola

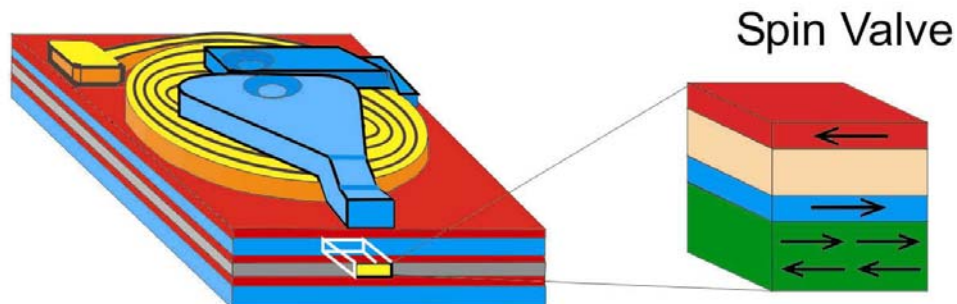
Applications: Giant Magnetoresistance



➡ = direction of magnetization

FM = Ferromagnet

Hard Drive Read Heads



Recent Research on Half Metals

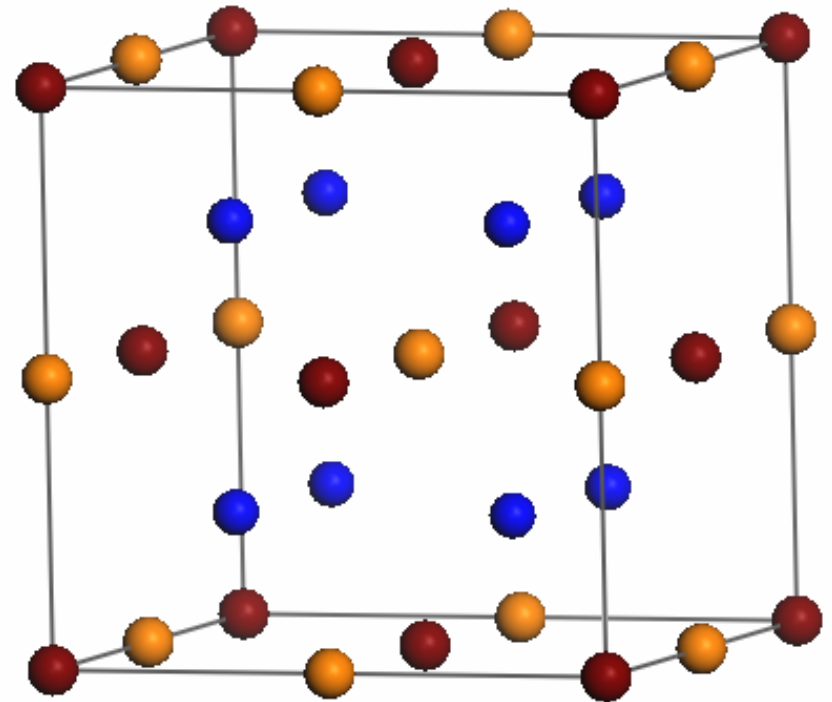
Material	T _c (K)	Polarization (%) by Point Contact Spectroscopy*	
Reference (Not Half-Metal)			
Co	1388	42	[Soulén et. al, Science 282, 85 (1998)]
Oxides			
La _{0.7} Sr _{0.3} MnO ₃	350	78	[Soulén et. al, Science 282, 85 (1998)]
CrO ₂	386	96	[Ji et.al, Phys. Rev. Lett., 86, 5585 (2001)]
Heusler Alloys			
NiMnSb	728	45	[Ritchie et. al, Phys. Rev. B 68, 104430 (2003)]
Co ₂ MnSi	1030	54	[Singh et. al, Appl. Phys. Lett., 29, 2367 (2004)]
Co ₂ MnGe	905	50-60	[Chen et. al , IEEE Trans. Magn. 37,2176 (2001)]

Half-Metallic Heusler Alloys

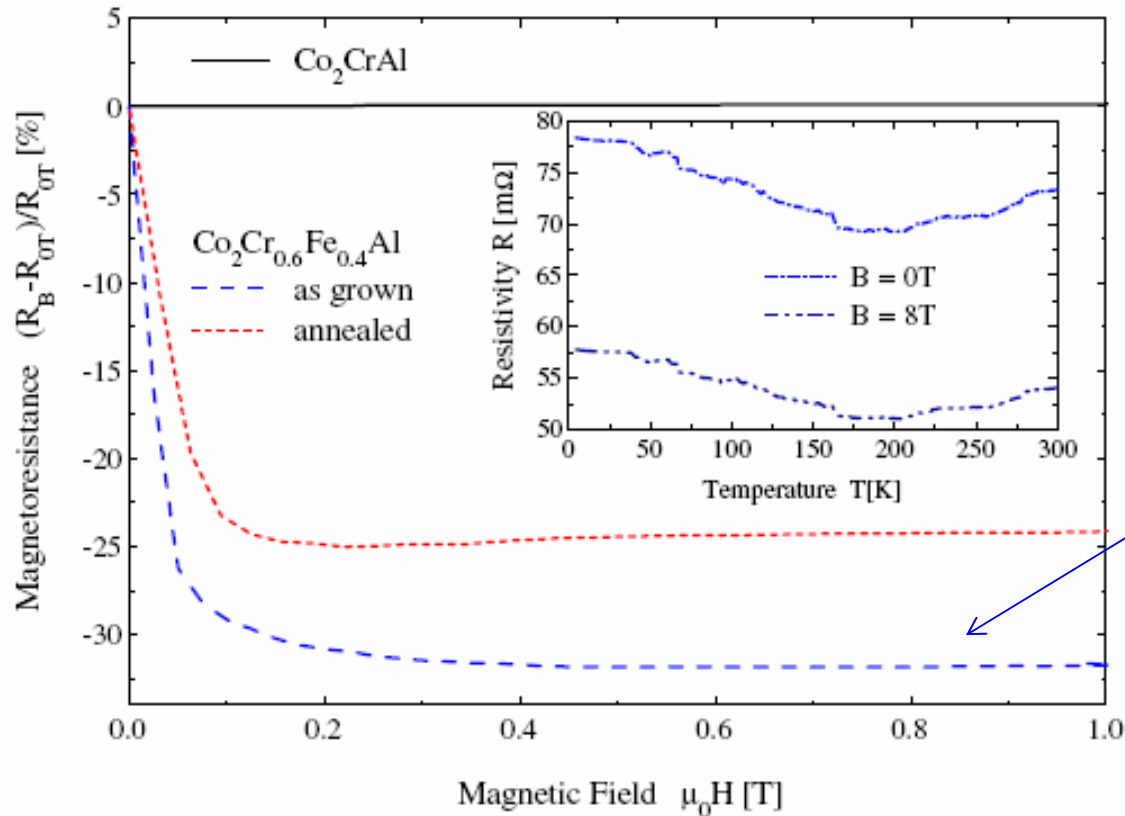
- High Curie temperatures
- Less demanding growth requirements
- Examples



L2_1 Structure



Room Temperature Magnetoresistance in Bulk Powder Compacts of Heusler Alloy $\text{Co}_2\text{Cr}_{0.6}\text{Fe}_{0.4}\text{Al}$



- Curie T of 650 K
- Largest magnetoresistance in a bulk metallic material at room T

Block et. al, J. Sol. State Chem. 176, 646 (2003)

DOS in $\text{Co}_2\text{Cr}_{1-x}\text{Fe}_x\text{Al}$

Half-metallicity in
 $\text{Co}_2\text{Cr}_{1-x}\text{Fe}_x\text{Al}$
 for low x ($x \leq 0.6$)

Elmers et. al, Phys. Rev. B 67, 104412
 (2003)

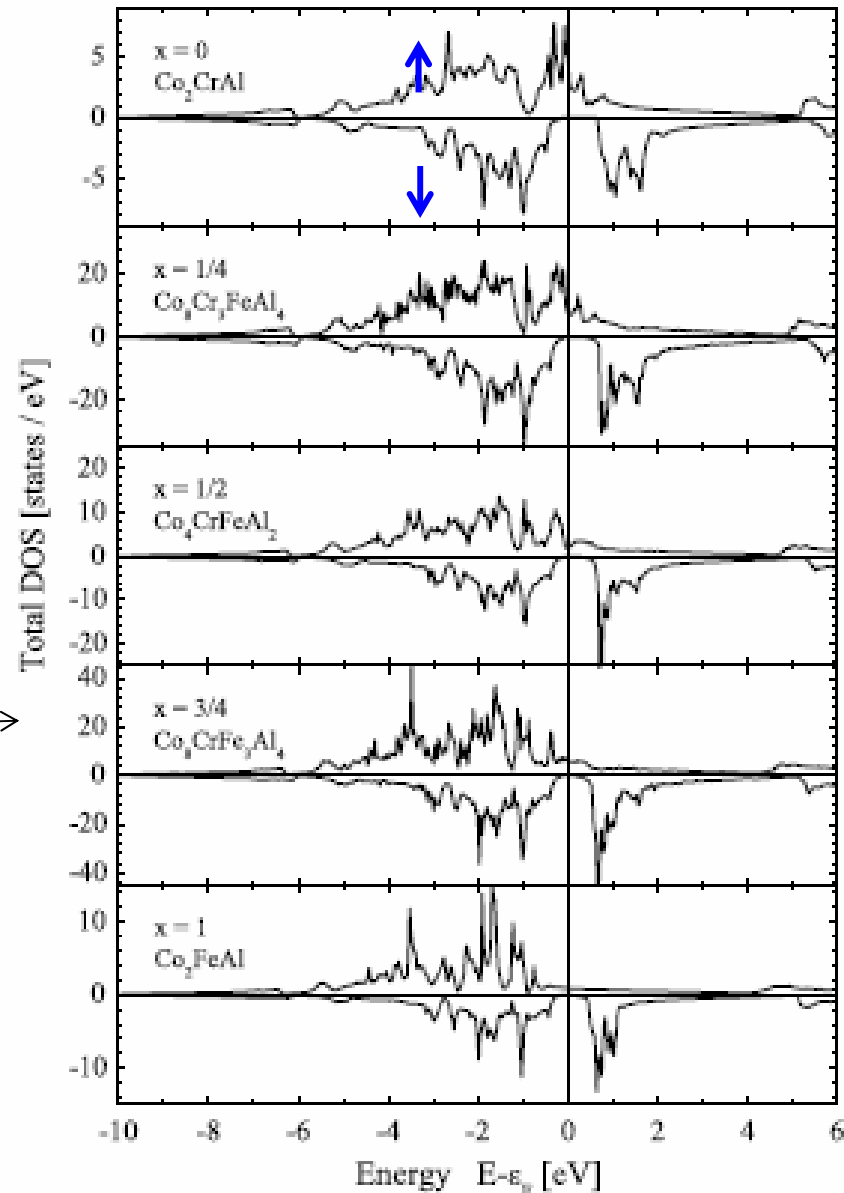
I. Galanakis, J. of Phys.: Cond. Matt.
16,3089 (2004)

Miura et. Al, Phys. Rev. B 69, 144413
 (2004)

Fecher et. Al, J. Phys. Cond. Matt 17,
 7237 (2005)

Antonov et. al, Phys. Rev. B 72,
 054441 (2005)

$M_s = 3 + 2x$ (holds for low x ,
 and approximately for high x ,
 in μ_B / f.u.)



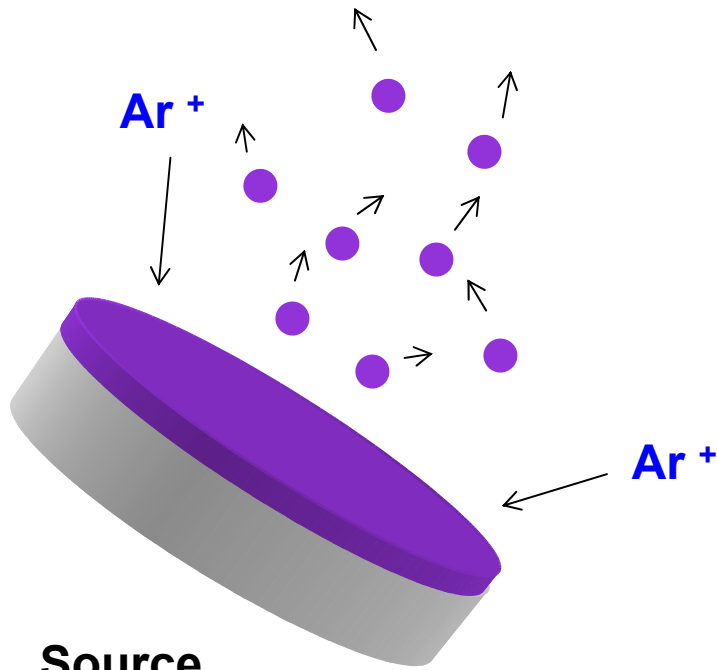
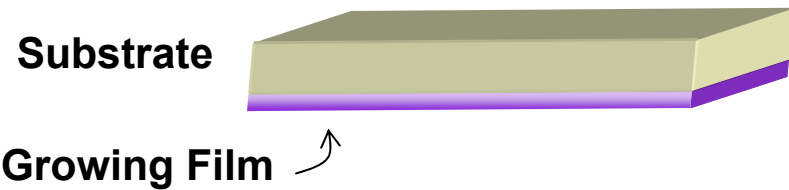
$\text{Co}_2\text{Cr}_{1-x}\text{Fe}_x\text{Al}$ Crystal Growth

- Singly Oriented Crystalline Samples → Intrinsic Properties
- In the bulk, neither Co_2CrAl nor Co_2FeAl have been grown as a single crystal
- In thin film growth
 - Single crystal substrate → single orientation
 - Can also investigate applications

Outline

- I. Description of Half Metals and Reasons For Studying $\text{Co}_2\text{Cr}_{1-x}\text{Fe}_x\text{Al}$
- II. Epitaxial Growth and Basic Characterization of $\text{Co}_2\text{Cr}_{1-x}\text{Fe}_x\text{Al}$
- III. Incorporation of Epitaxial $\text{Co}_2\text{Cr}_{1-x}\text{Fe}_x\text{Al}$ into Superlattices and Spin Valves
- IV. Electronic and Magnetic Properties of Single-Layer Epitaxial Films
 - A. Measurement of the Spin Polarization
 - B. Study of the Elemental Magnetic Moments
 - C. Quantifying Atomic Disorder
- V. Conclusions

Growth of Epitaxial $\text{Co}_2\text{Cr}_{1-x}\text{Fe}_x\text{Al}$



- Substrate

MgO (001) ~ 4% mismatch

also MgAl_2O_4 , Si

- Growth Temperature

500°C (chosen for structural and magnetic properties)

- Targets

High Purity Al, Fe, Co, Cr

- Capped with Al or SiC

Basic Characterization of Epitaxial Films

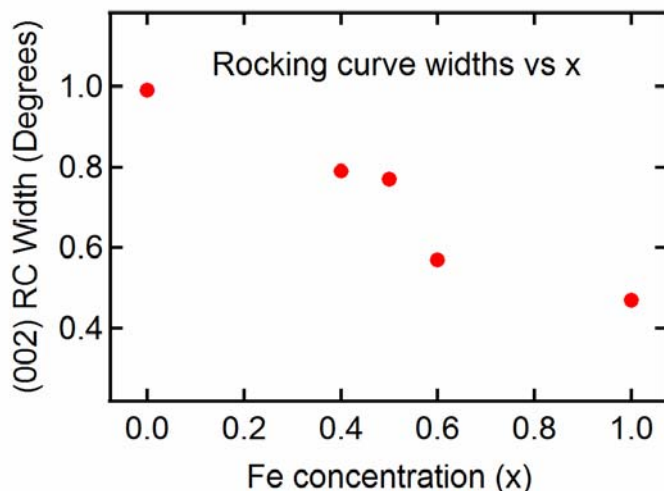
- Phases present and crystalline orientation – X-ray diffraction
- Composition -- Rutherford Backscattering Spectrometry (RBS) and Electron Microprobe Analysis (EPMA)
- Thickness and Surface Roughness – X-ray Reflectivity

High Angle X-ray Diffraction of $\text{Co}_2\text{Cr}_{1-x}\text{Fe}_x\text{Al}$

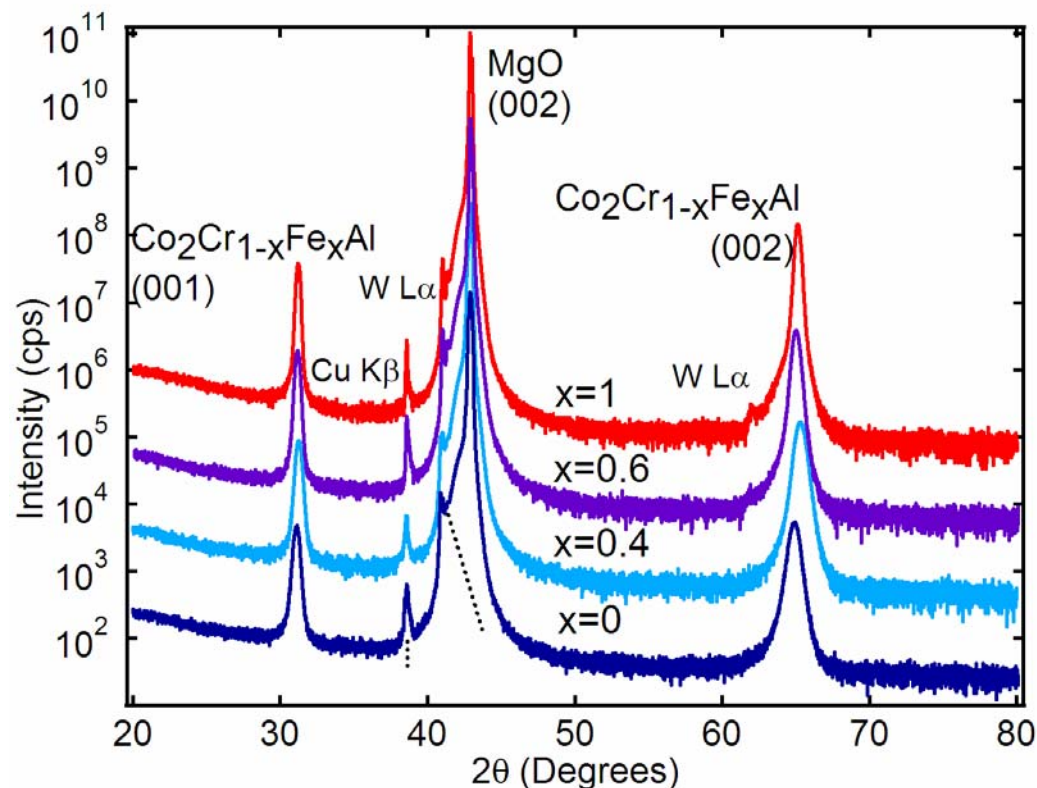
High Angle X-ray Diffraction

- Single phase
- Singly oriented

Rocking Curve FWHMs

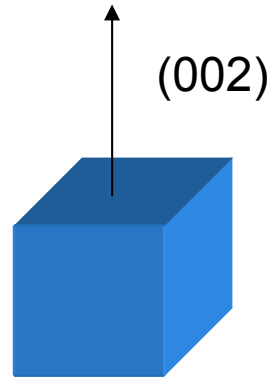


High Angle X-ray Diffraction of 1000 Å Films

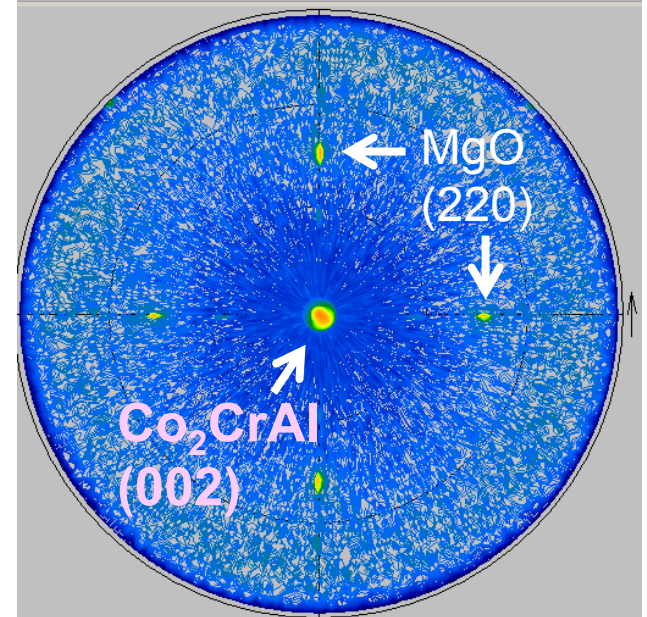
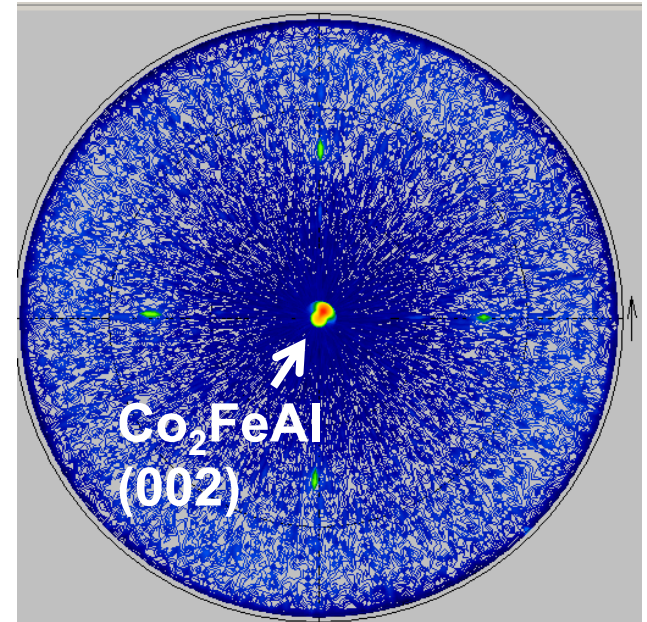
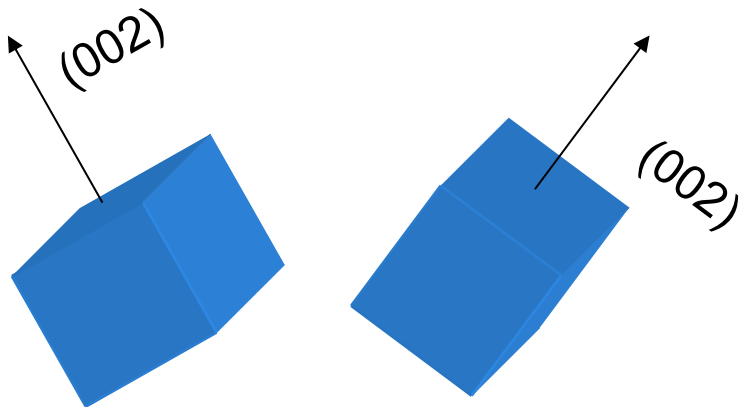


Single Orientation

- Pole Figures show the (002) oriented along a single direction

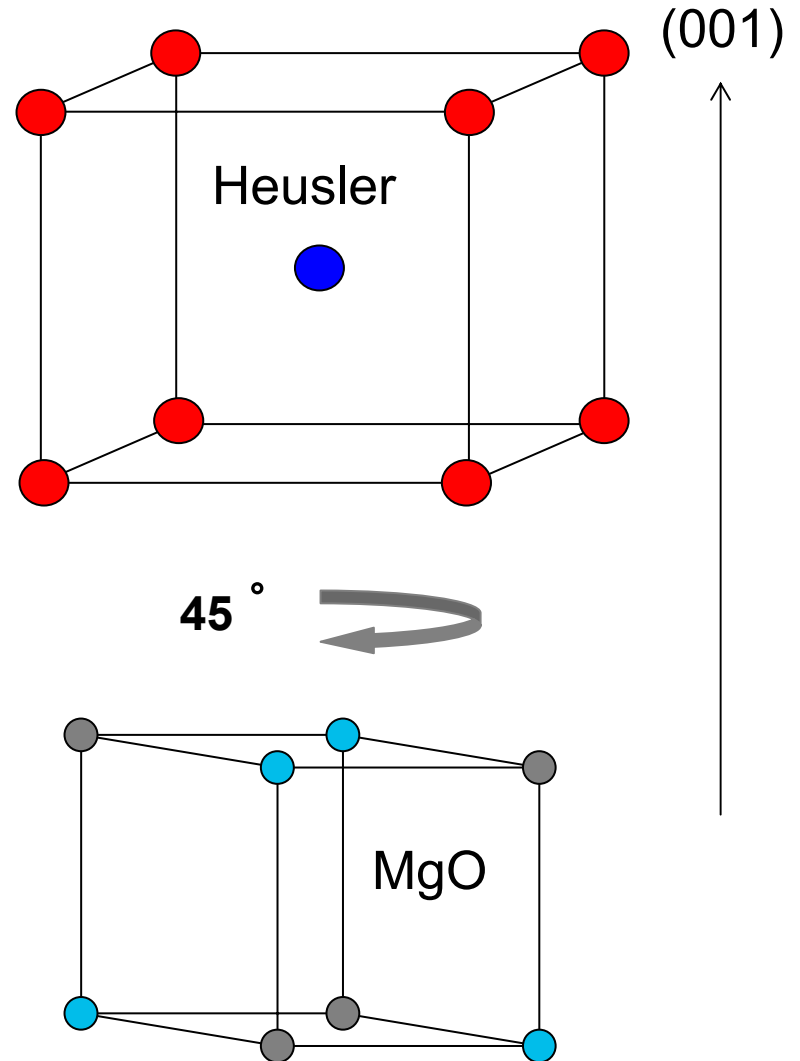
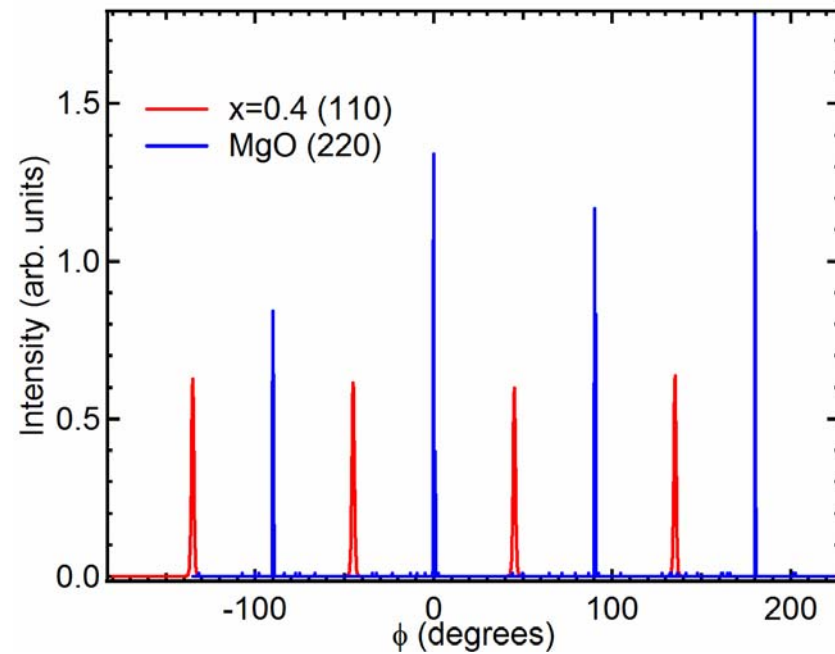


- No orientations like below



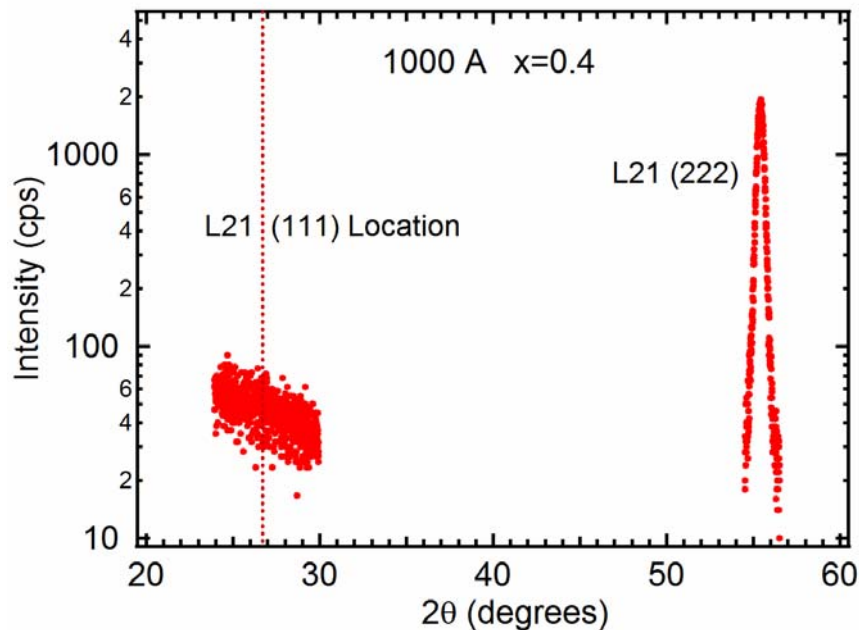
In-Plane Orientation

Typical Phi Scan of MgO and Heusler, for $x=0.4$



B2 Disorder in $\text{Co}_2\text{Cr}_{1-x}\text{Fe}_x\text{Al}$

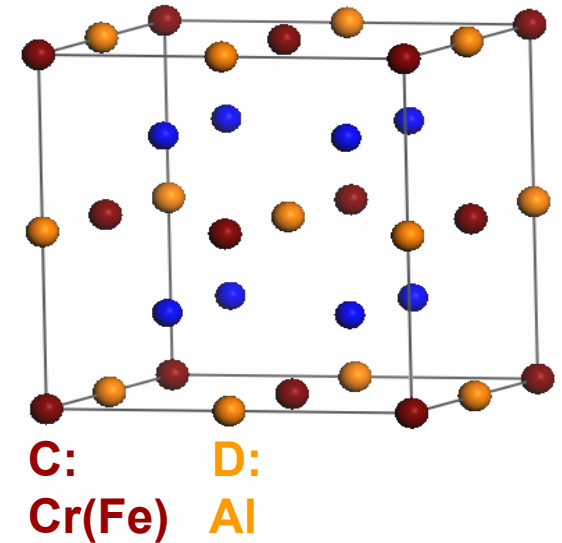
- Missing $L2_1$ (111) peak implies higher symmetry crystal structure
- Similar to bulk



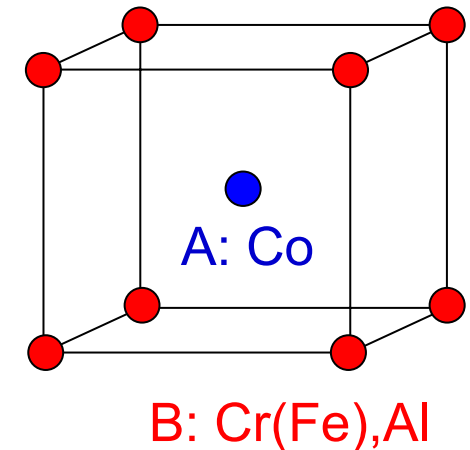
$$F_{111} = 4 |f_{\text{C}} - f_{\text{D}}|$$

$$F_{222} = 4 |f_{\text{C}} + f_{\text{D}}|$$

$L2_1$

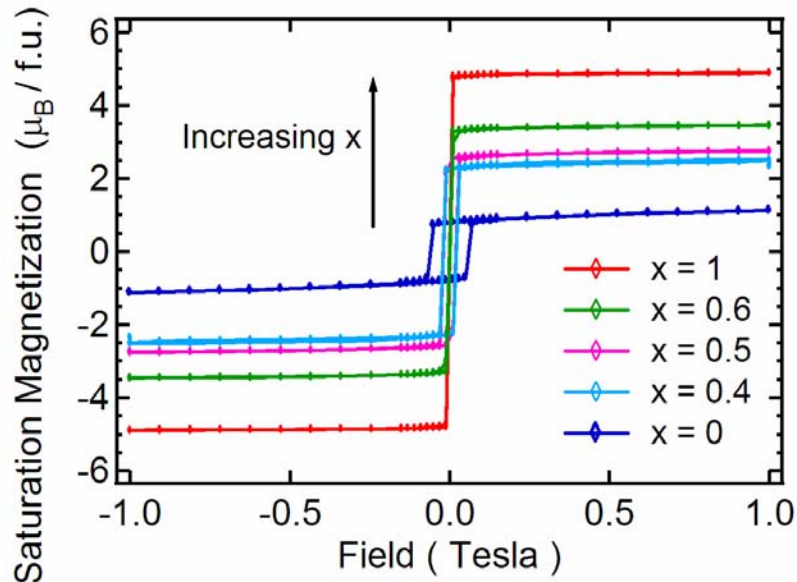


B2



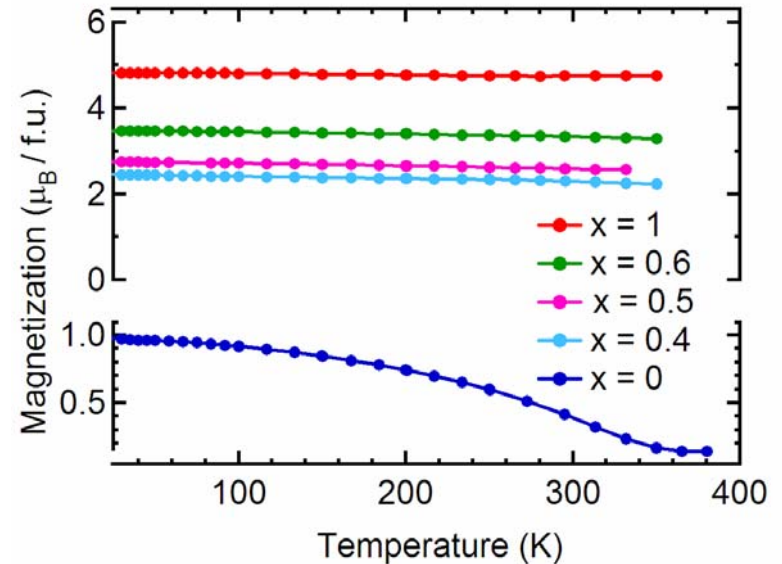
$\text{Co}_2\text{Cr}_{1-x}\text{Fe}_x\text{Al}$ Magnetization

M vs H at 5 Kelvin, along [110]



- Magnetization increases with x
- Higher coercivity in low x results from higher structural disorder

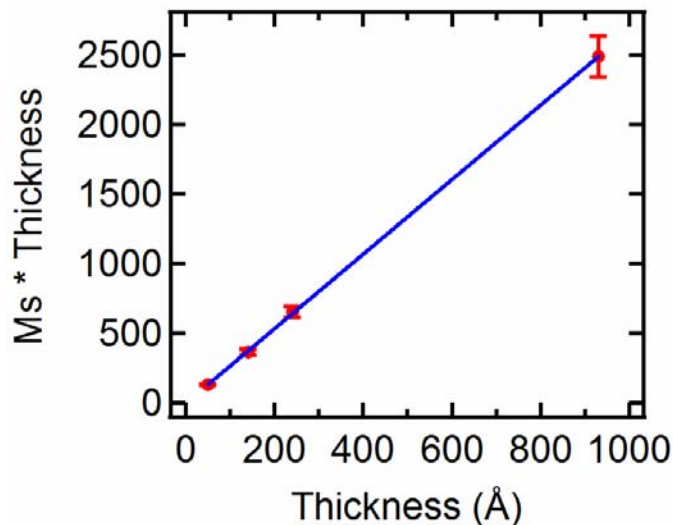
M vs T in 5000 Oe, along [110]



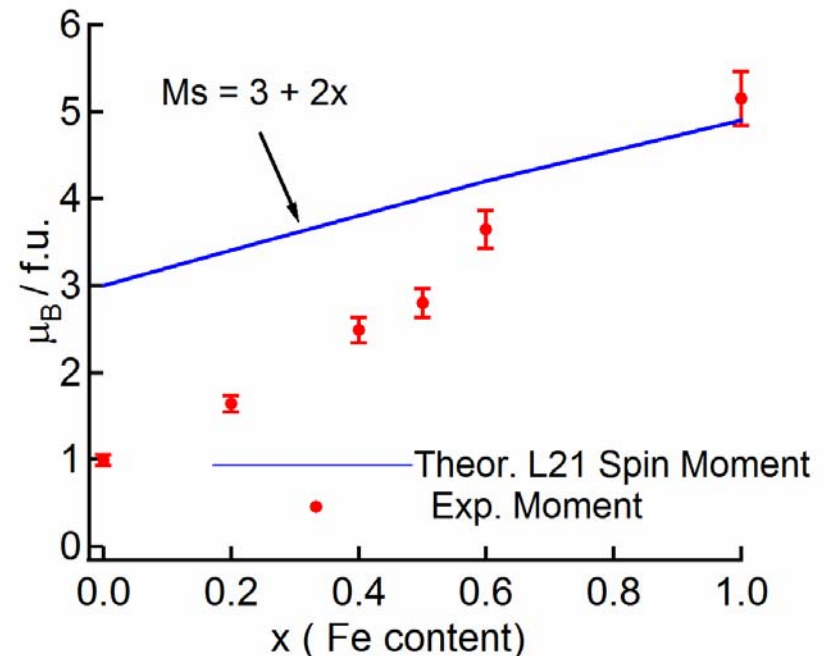
- High T_c in $x > 0$
- $T_c \sim 370\text{-}380$ K in $x=0$

Magnetization vs Thickness and Composition of $\text{Co}_2\text{Cr}_{1-x}\text{Fe}_x\text{Al}$

- Films homogeneous down to 50 Å



- Reduction of magnetization for low Fe concentration x



Outline

- I. Description of Half Metals and Reasons For Studying $\text{Co}_2\text{Cr}_{1-x}\text{Fe}_x\text{Al}$
- II. Epitaxial Growth and Basic Characterization of $\text{Co}_2\text{Cr}_{1-x}\text{Fe}_x\text{Al}$
- III. Incorporation of Epitaxial $\text{Co}_2\text{Cr}_{1-x}\text{Fe}_x\text{Al}$ into Superlattices and Spin Valves
- IV. Electronic and Magnetic Properties of Single-Layer Epitaxial Films
 - A. Measurement of the Spin Polarization
 - B. Study of the Elemental Magnetic Moments
 - C. Quantifying Atomic Disorder
- V. Conclusions

Superlattices and Spin Valves of $\text{Co}_2\text{Cr}_{1-x}\text{Fe}_x\text{Al}$

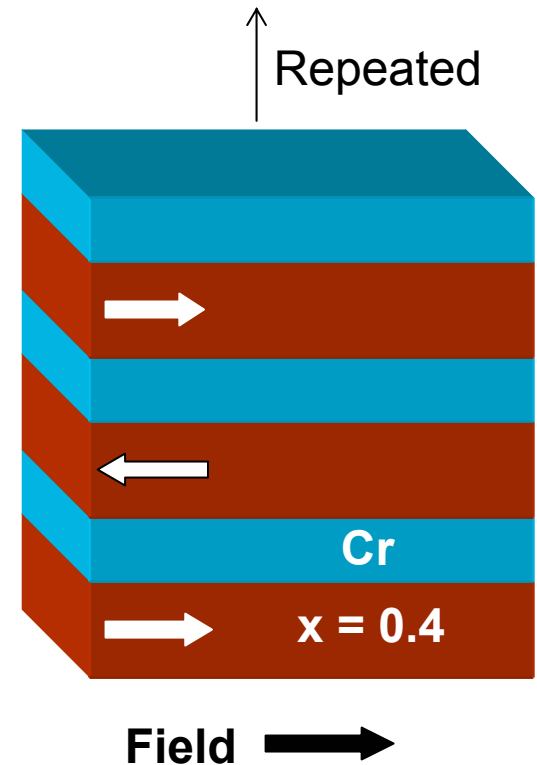
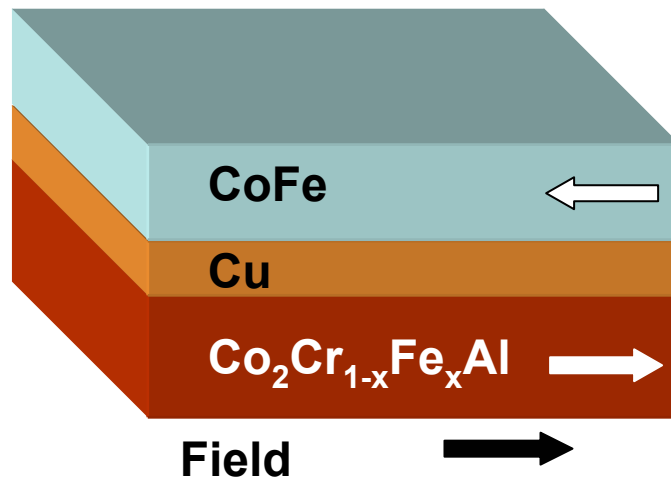
Structures for current in plane
giant magnetoresistance applications

- Multilayers with Cr for $x=0.4$

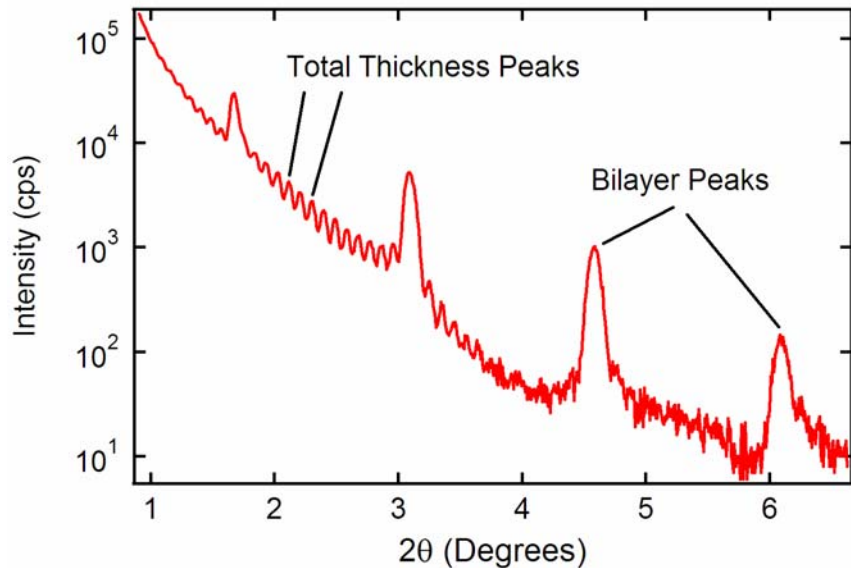
Both are cubic

$$a_{\text{Cr}} = 2.88 \text{ \AA} \leftrightarrow a_{\text{Heusler}} = 2.87 \text{ \AA}$$

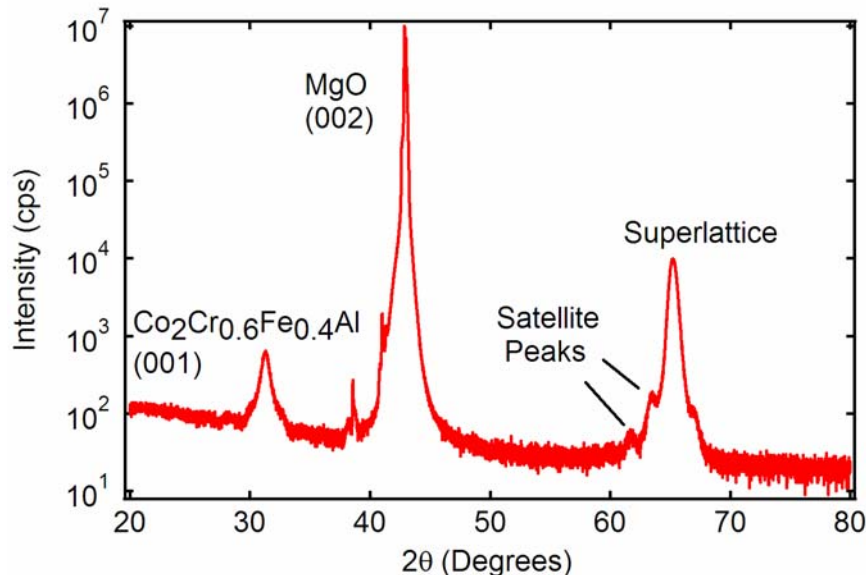
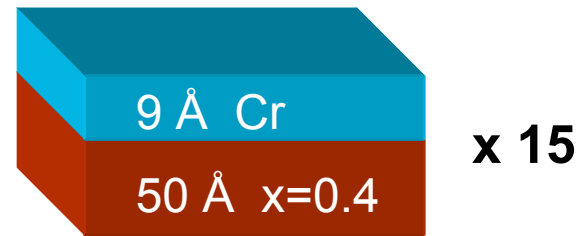
- Spin valves



Growth of Superlattices

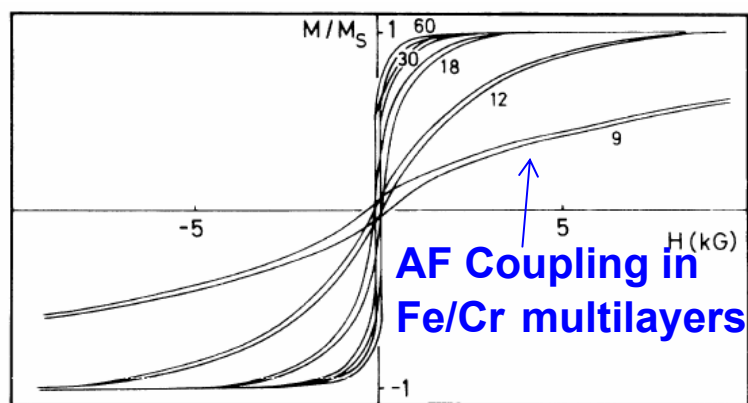
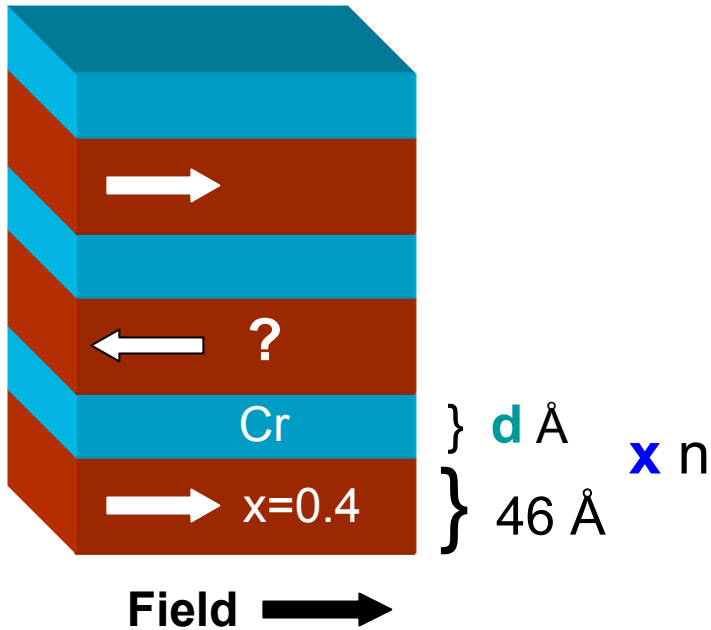


- Grown at 350°C
- Reflectivity \rightarrow roughness ~ 1 monolayer

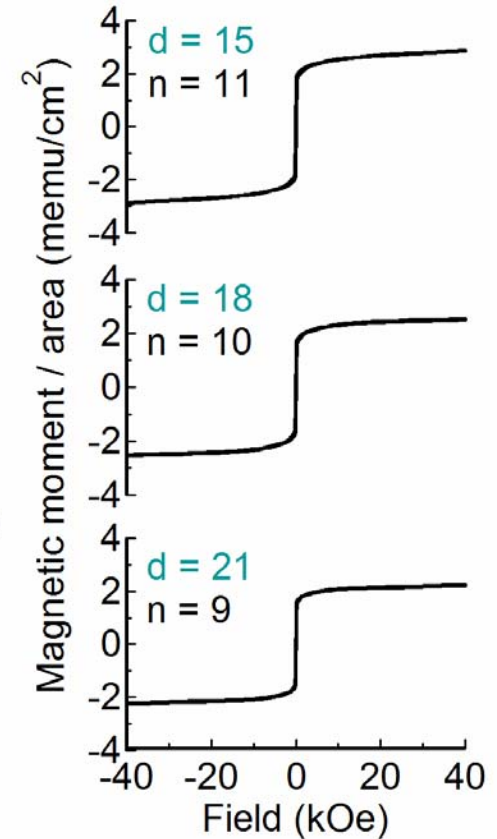
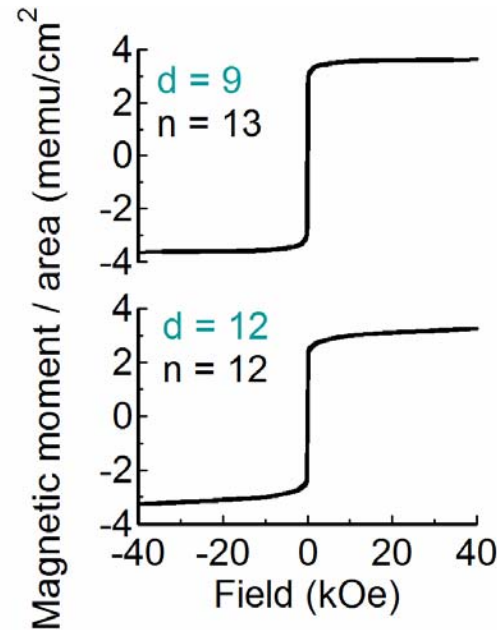


- Satellite peaks \rightarrow bilayer periodicity
- Phi scans \rightarrow cube on cube growth for Heusler and Cr

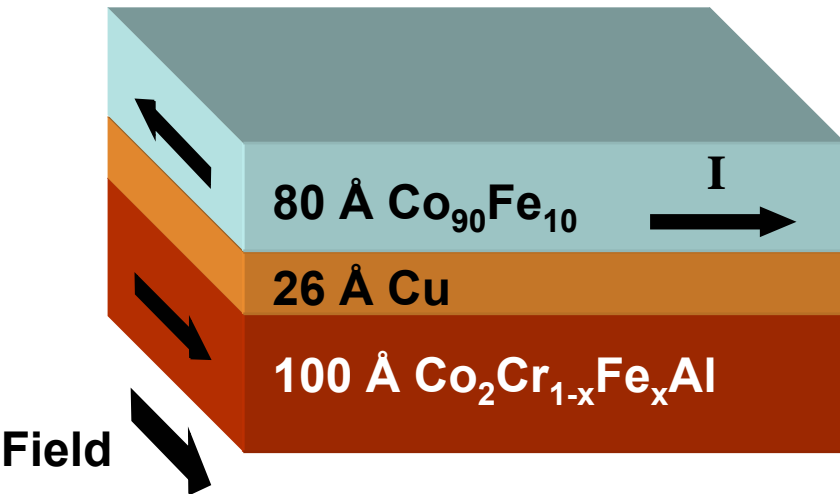
No Evidence for Antiferromagnetic Coupling



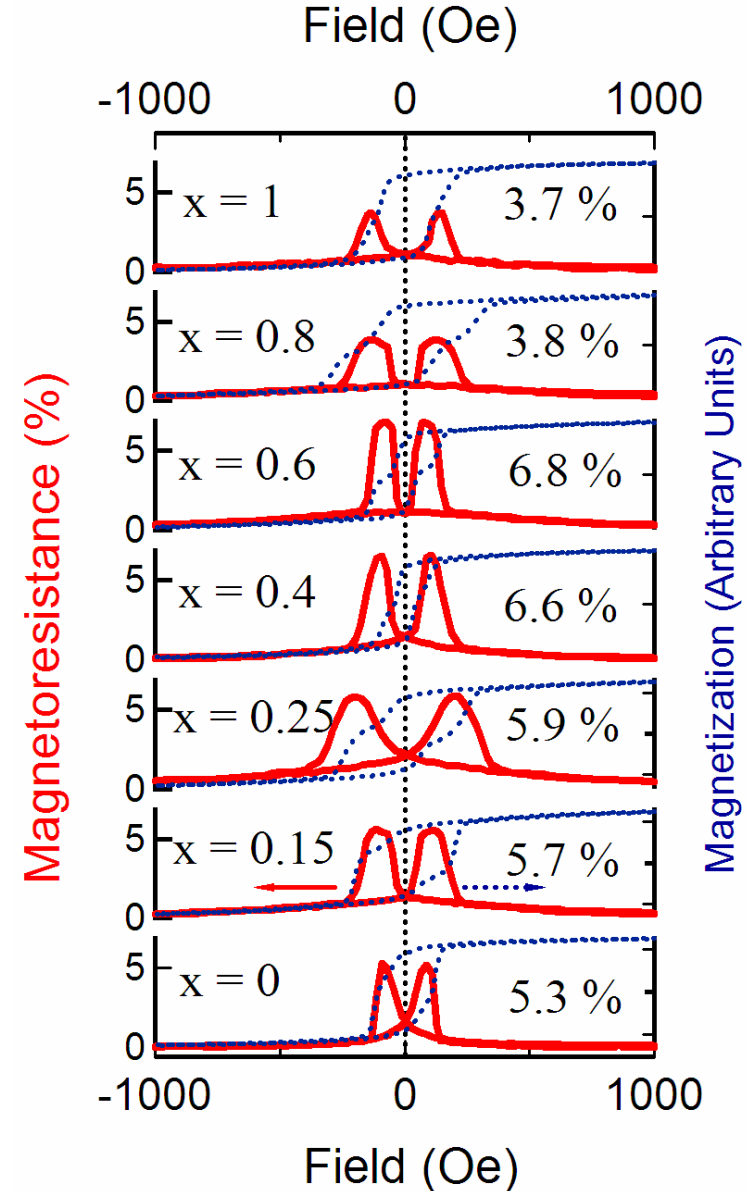
Baibich et. al, Phys. Rev. Lett. 61, 2472 (1988)



Giant Magnetoresistance at Room T



- No exchange biasing layer
- Similar results for Field // I
- Trilayers grown on glass show 10x smaller GMR
- Comparable to conventional spin valves



Comparison with other predicted half metals

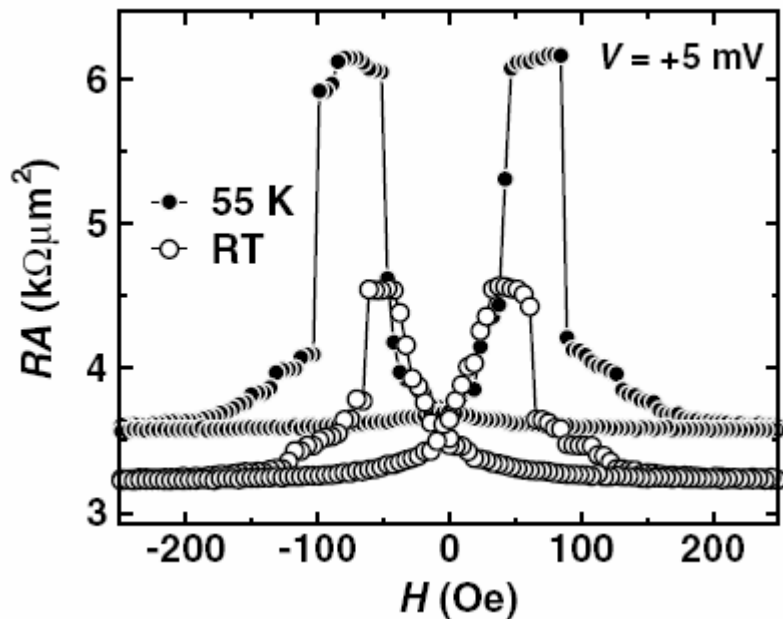
- First demonstration of large ($\sim 7\%$) giant magnetoresistance in a theoretical half metal
- Addition of exchange biasing layer and further optimization should yield even larger values
- Order of magnitude larger than spin valves with other predicted half metals

PtMnSb	0.47 %	Johnson et. al, IEEE TRANS. ON MAGN. 32, 4615 (1996)
NiMnSb	1% at 60 K	Hordequin et. al, J. Magn. Mat. 183, 225 (1998)
Co₂MnGe	0.2%	Ambrose et. al, J. Appl. Phys. 89, 7522 (2001)
CrO₂	0.2 %	Miao et. Al, J. Appl. Phys. 97, 10C924 (2005)

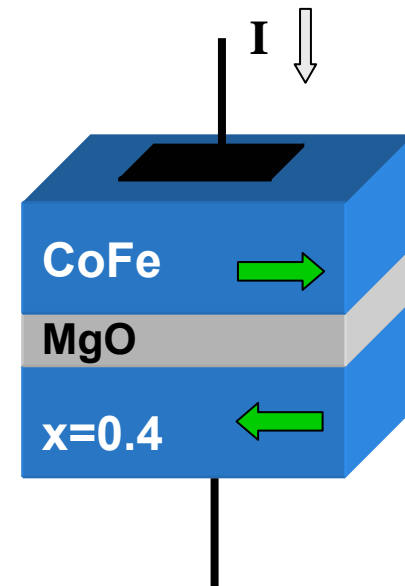
Recent Results on Tunneling Magnetoresistance in $\text{Co}_2\text{Cr}_{1-x}\text{Fe}_x\text{Al}$

Employing methods similar to ours, Yamamoto et. al recently grew epitaxial films of $x=0.4$ on MgO \rightarrow tunnel junctions

TMR of 42% at RT and 74% at 55 K



Current flows **perpendicular to plane**



Yamamoto et. al, J. Phys. D 39,
824 (2006)

Large Magnetoresistances Motivation for Further Study

- Results from spin valve trilayers indicate promise of $\text{Co}_2\text{Cr}_{1-x}\text{Fe}_x\text{Al}$ for applications
- Motivate further study of:
Electronic and Magnetic Properties

Outline

- I. Description of Half Metals and Reasons For Studying $\text{Co}_2\text{Cr}_{1-x}\text{Fe}_x\text{Al}$
- II. Epitaxial Growth and Basic Characterization of $\text{Co}_2\text{Cr}_{1-x}\text{Fe}_x\text{Al}$
- III. Incorporation of Epitaxial $\text{Co}_2\text{Cr}_{1-x}\text{Fe}_x\text{Al}$ into Superlattices and Spin Valves
- IV. Electronic and Magnetic Properties of Single-Layer Epitaxial Films
 - A. Measurement of the Spin Polarization
 - B. Study of the Elemental Magnetic Moments
 - C. Quantifying Atomic Disorder
- VI. Conclusions

Point Contact Andreev Reflection (PCAR) Spectroscopy

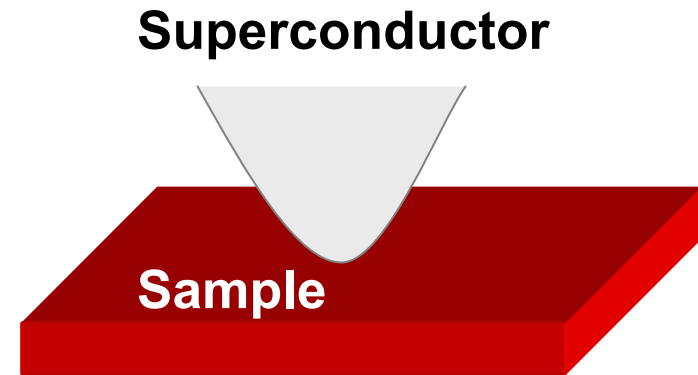
- Measure conductance as a function of applied voltage bias

Actually measuring

$$P_c = \frac{I_{\uparrow} - I_{\downarrow}}{I_{\uparrow} + I_{\downarrow}},$$

rather than

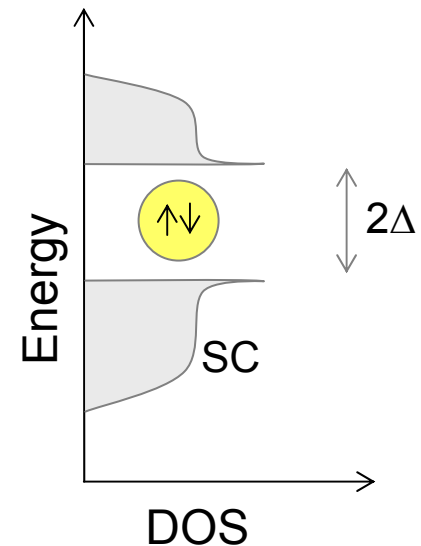
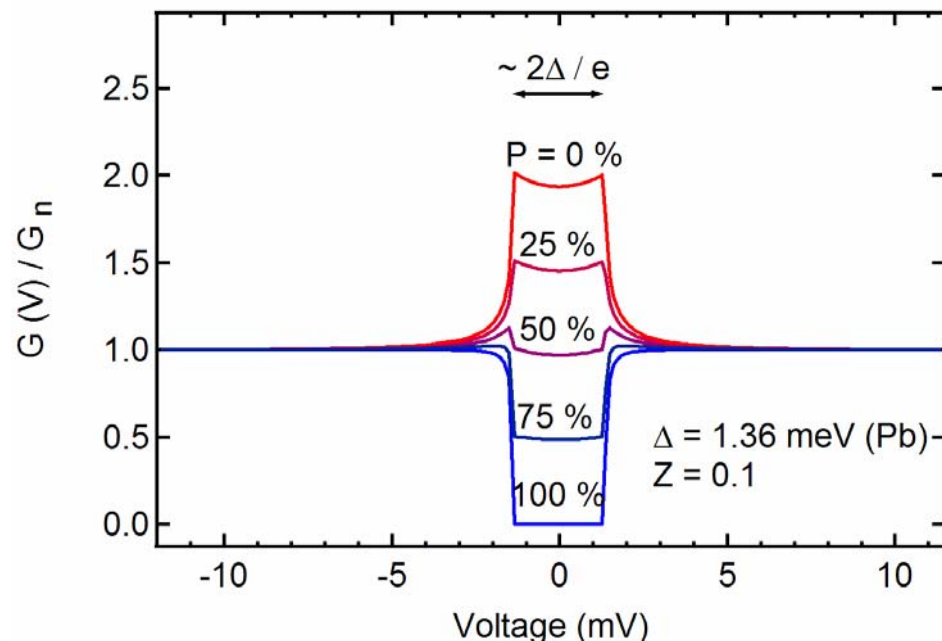
$$P = \frac{n_{\uparrow} - n_{\downarrow}}{n_{\uparrow} + n_{\downarrow}}$$



Soulen et. al, Science 282, 85 (1998)

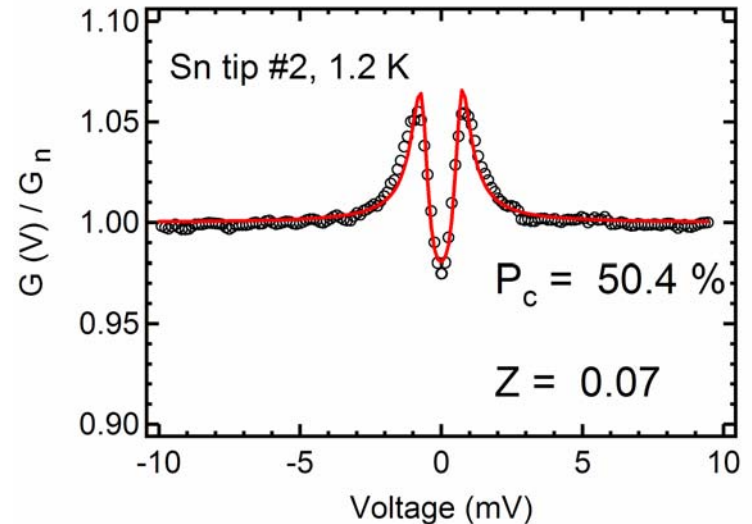
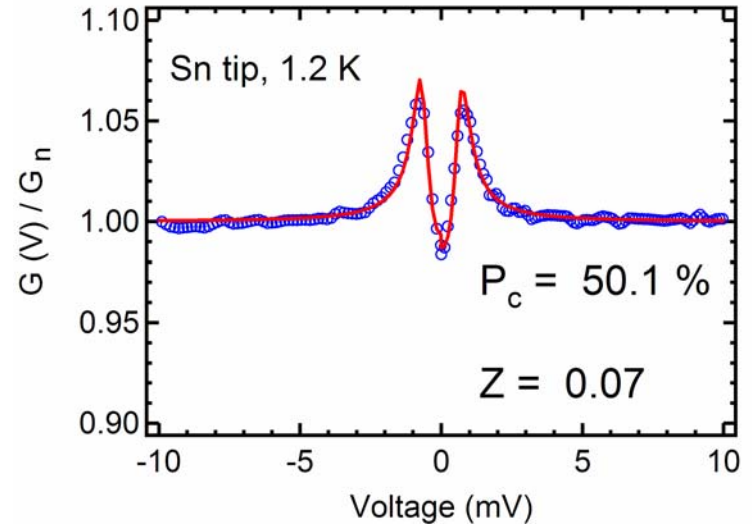
Effect of P_c on the conductance

- Blonder et. al \rightarrow first theory, included interfacial scattering Z [Blonder et. al, Phys. Rev. B 25, 4515 (1982)]
- Mazin et. al modified the theory to account for half metals [Mazin et. al, J. Appl. Phys. 89, 7576 (2001)]

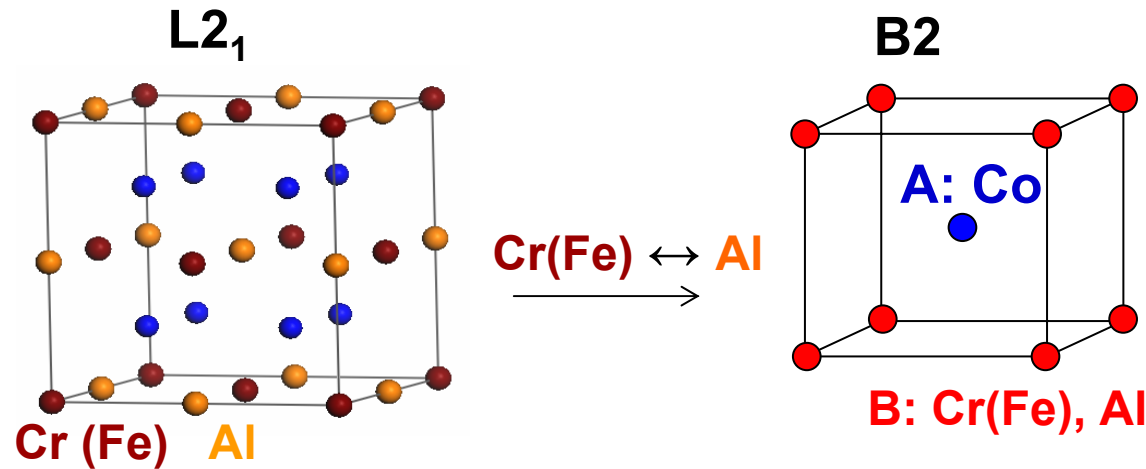
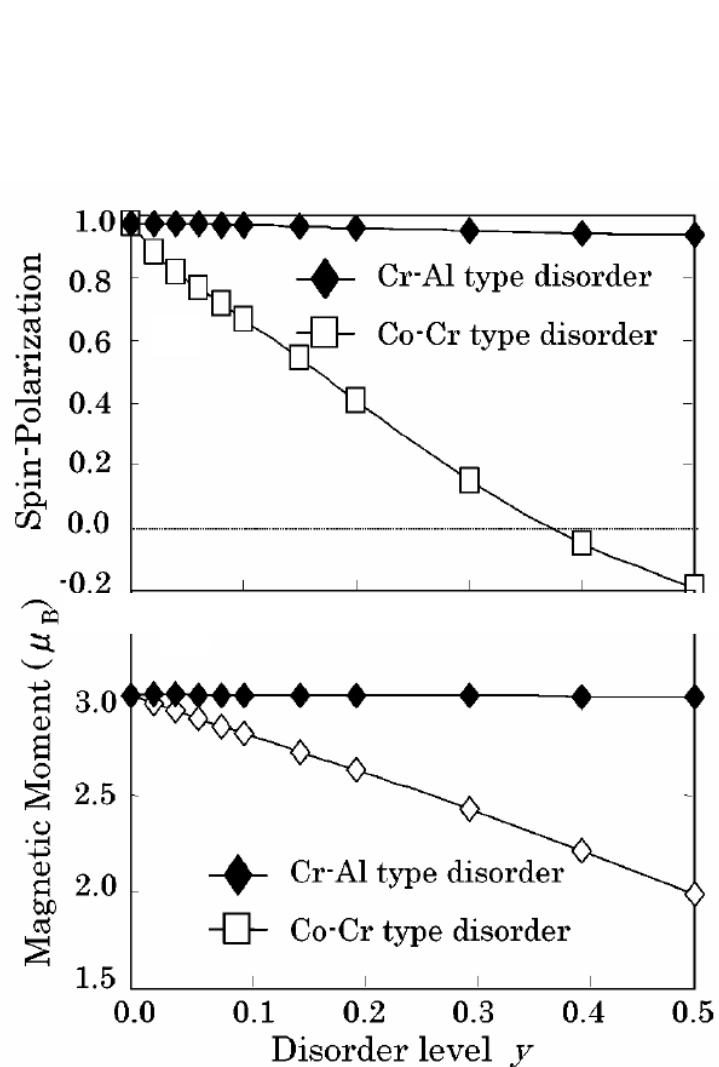


Point Contact Andreev Reflection Spectroscopy (PCAR)

- Measured P_c of $\text{Co}_2\text{Cr}_{0.6}\text{Fe}_{0.4}\text{Al}$ with ~ 30 different contacts
- 3 fitting parameters:
 P_c , Z , R_s
- Average P_c of 50%

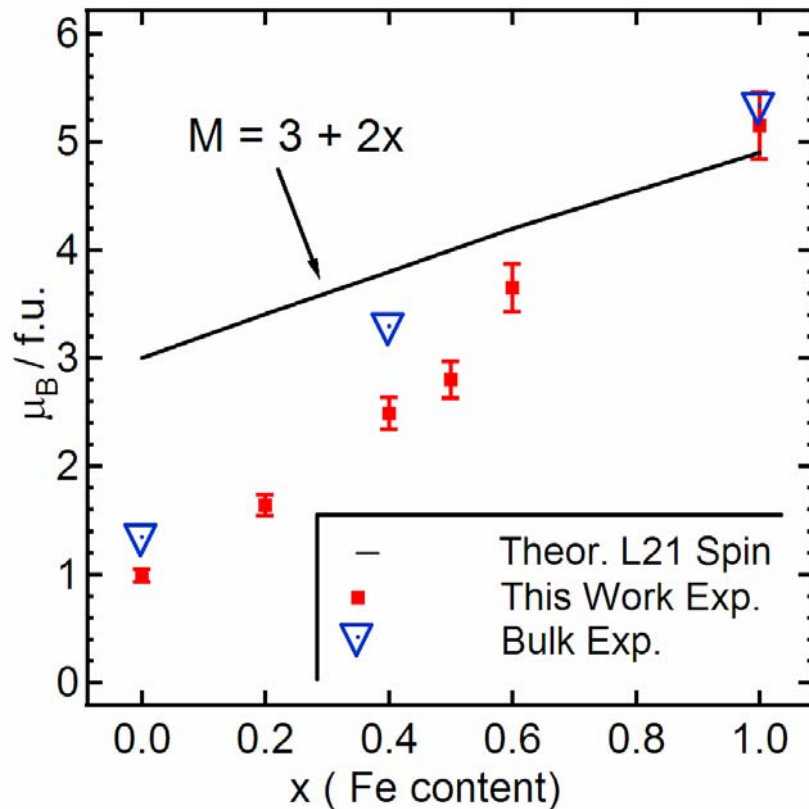


Effect of B2 Disorder on Spin Polarization of $\text{Co}_2\text{Cr}_{1-x}\text{Fe}_x\text{Al}$



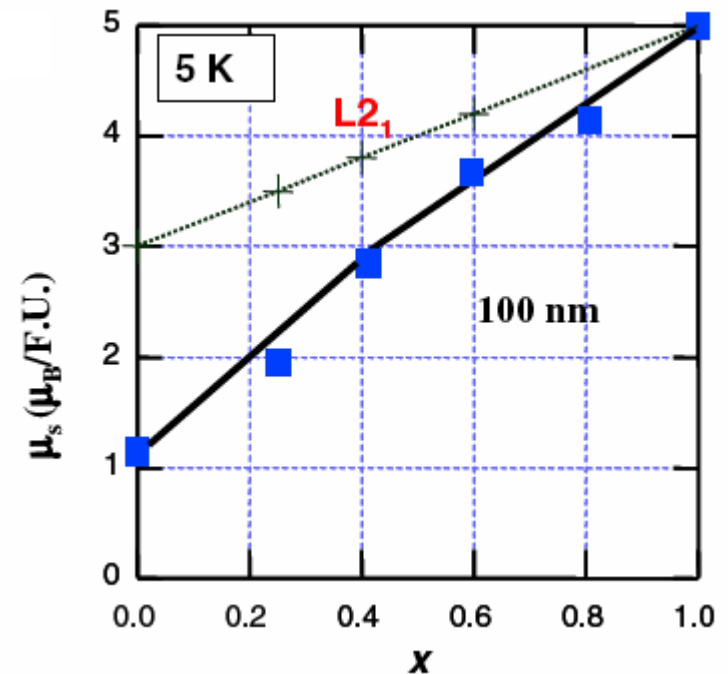
- Effect on Co_2CrAl
- Similar results for $\text{Co}_2\text{Cr}_{1-x}\text{Fe}_x\text{Al}$
- Co disorder significantly affects spin polarization and magnetization

Spin Polarization and Reduction of Moment



Bulk values from Felser et. al, J. of Phys. Cond. Matt. 15, 7019 (2003) and Wurmehl et. al J. Phys. D 39, 803 (2006).

Inomata et. al have reproduced our results for epitaxial films on MgO



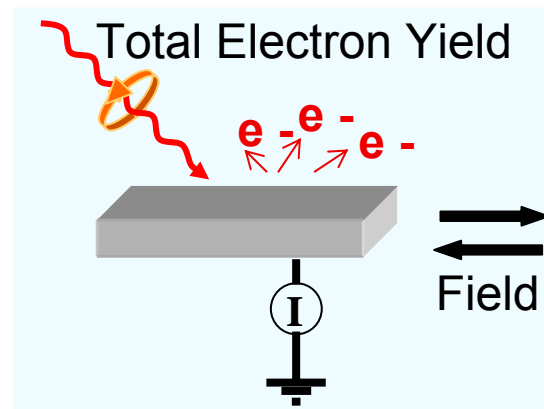
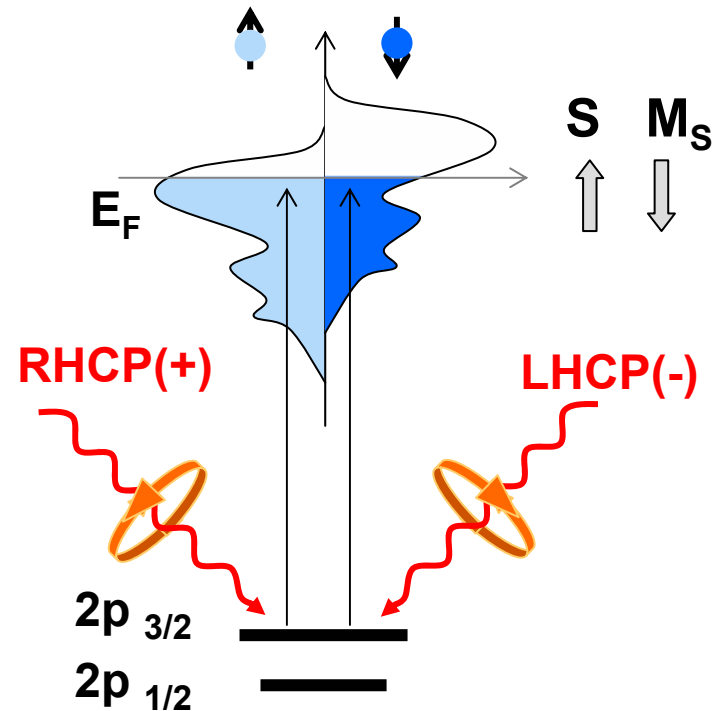
Inomata et al. J. Phys. D: Appl. Phys. 39, 816 (2006).

Outline

- I. Description of Half Metals and Reasons For Studying $\text{Co}_2\text{Cr}_{1-x}\text{Fe}_x\text{Al}$
- II. Epitaxial Growth and Basic Characterization of $\text{Co}_2\text{Cr}_{1-x}\text{Fe}_x\text{Al}$
- III. Incorporation of Epitaxial $\text{Co}_2\text{Cr}_{1-x}\text{Fe}_x\text{Al}$ into Superlattices and Spin Valves
- IV. Electronic and Magnetic Properties of Single-Layer Epitaxial Films
 - A. Measurement of the Spin Polarization
 - B. Study of the Elemental Magnetic Moments
 - C. Quantifying Atomic Disorder
- V. Conclusions

Xray Magnetic Circular Dichroism

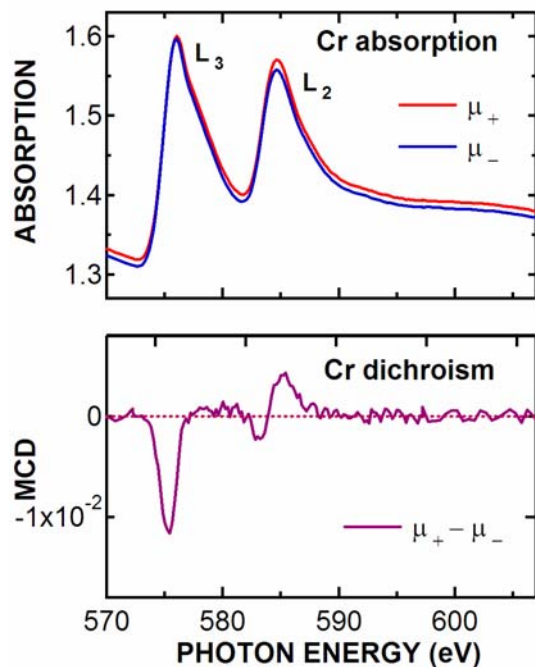
- Difference in absorption between RHCP(+) and LHCP(-) x-rays
- Study m_{orb} and m_{spin}
- We studied L_3 and L_2 edges (originating from $2p_{3/2}$ and $2p_{1/2}$) of Cr, Fe, and Co



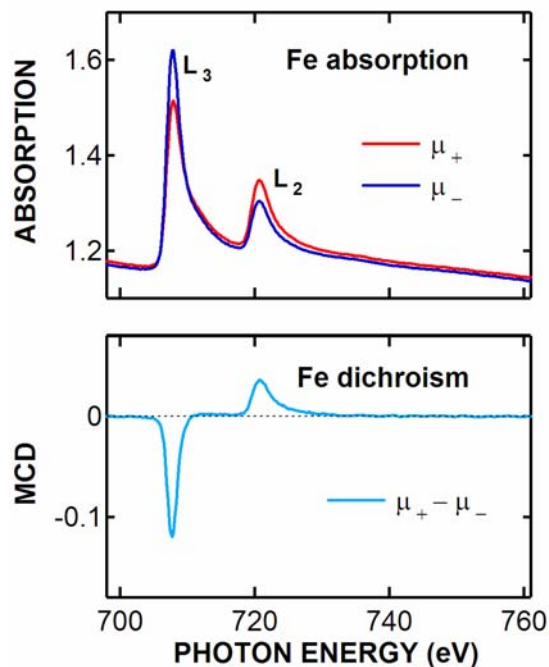
Representative Cr, Fe, and Co dichroism

- Cr dichroism shows small ferromagnetically aligned moment, and change of sign near L_2 edge

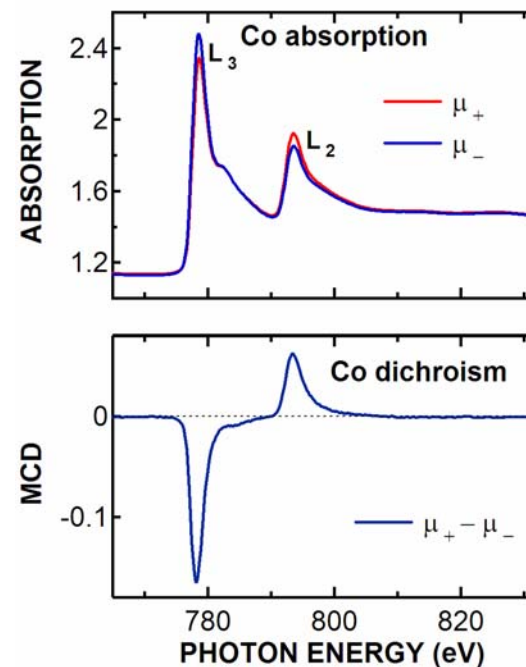
Cr



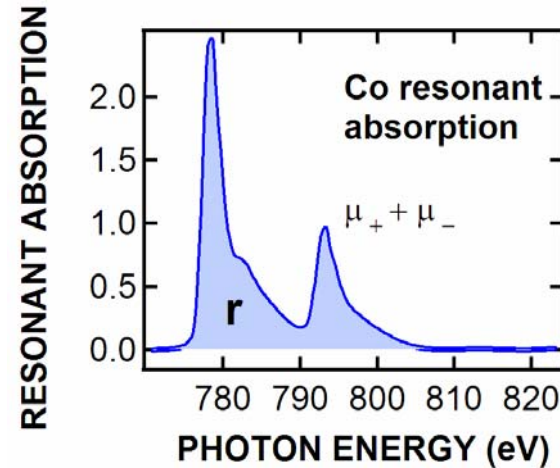
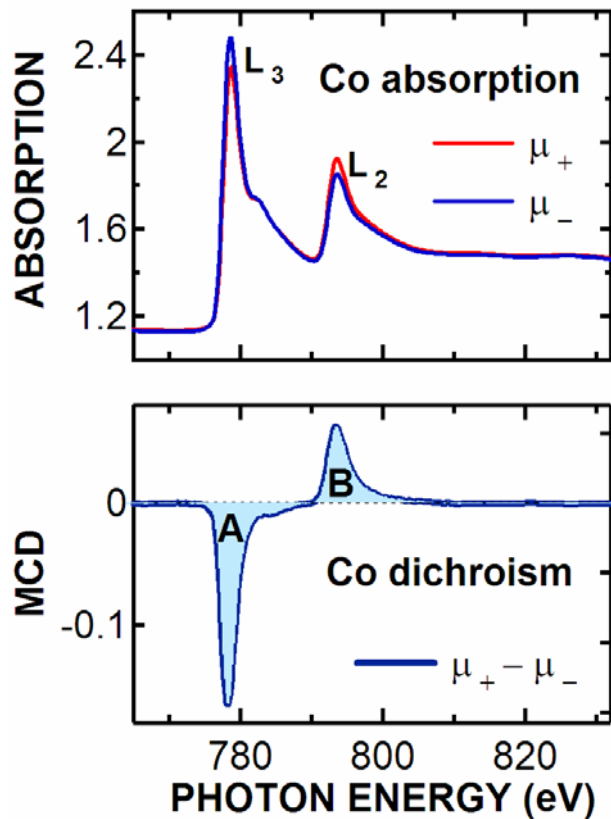
Fe



Co



Extraction of Moments



- **Magneto-optical sum rules** [Carra et. al, Phys. Rev. Lett. 70, 694 (1993) and Thole et. al, Phys. Rev. Lett. 68, 1943 (1992)]

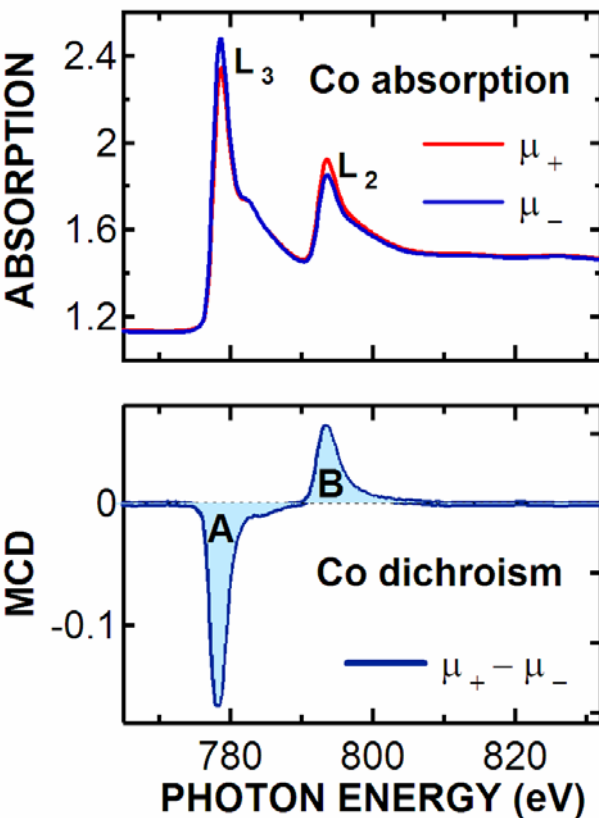
$$m_{\text{orb}} \sim \frac{(A + B)N_d}{r}$$

$$m_{\text{spin}} \sim \frac{(A - 2B)N_d}{r}$$

- We modified the sum rules

$N_d / r = C$, roughly constant for 1st row d elements (Cr, Fe, Co)

Modified Sum Rules



$$q = \int_{L_3+L_2} (\mu_+ - \mu_-) dE$$

$$p = \int_{L_3} (\mu_+ - \mu_-) dE \quad \text{Non-resonant excitation}$$

$$r = \int_{L_3+L_2} [(\mu_+ + \mu_-) - S] dE$$

$$m_{orb} = -4qN_h/3rP \cos \theta \quad \text{Angle btw photon k and B}$$

Beam polarization

Number of d holes

$$m_{spin} = -G(4q - 6p)N_h/rP \cos \theta \quad \begin{matrix} G = 1 \text{ (Fe, Co)} \\ G = 2 \text{ (Cr)} \end{matrix}$$

$$r_i = CN_{h,i}W_i \quad C = \text{const. (for transition metals)}$$

Measure
 $q \quad p \quad M_s$

Extract
 $m_{orb} \quad m_{spin}$

$$m_{orb,i} = \frac{-4q_i}{3W_iCP \cos \theta} \quad m_{spin,i} = \frac{-G_i(4q_i - 6p_i)}{W_iCP \cos \theta}$$

Measure
 $r \quad P \cos \theta$

Extract
 N_h

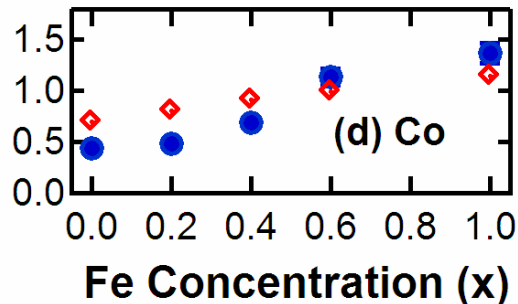
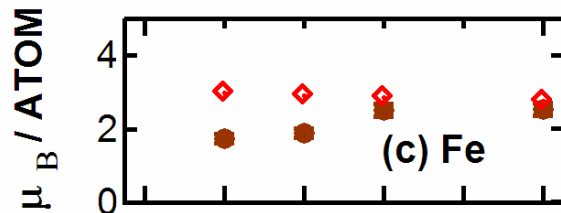
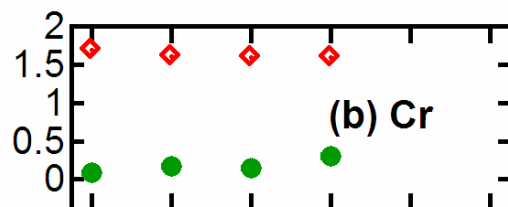
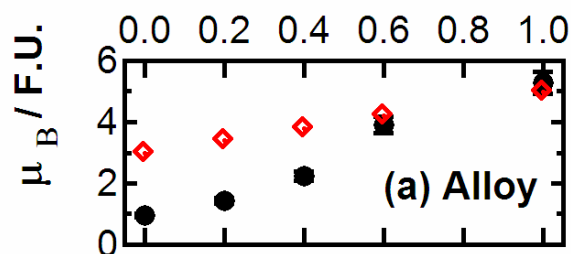
$$\sum_i (m_{orb,i} + m_{spin,i})W_i = M_s$$

Find $CP \cos \theta$ from saturation magnetization

Moments vs Composition

Spin Moments vs Composition

◇ L21 theory



Orbital moments small

$$m_{\text{orb}}(\text{Cr}) \sim 0 \mu\text{B} / \text{atom}$$

$$m_{\text{orb}}(\text{Fe}) \sim 0.1 \mu\text{B} / \text{atom}$$

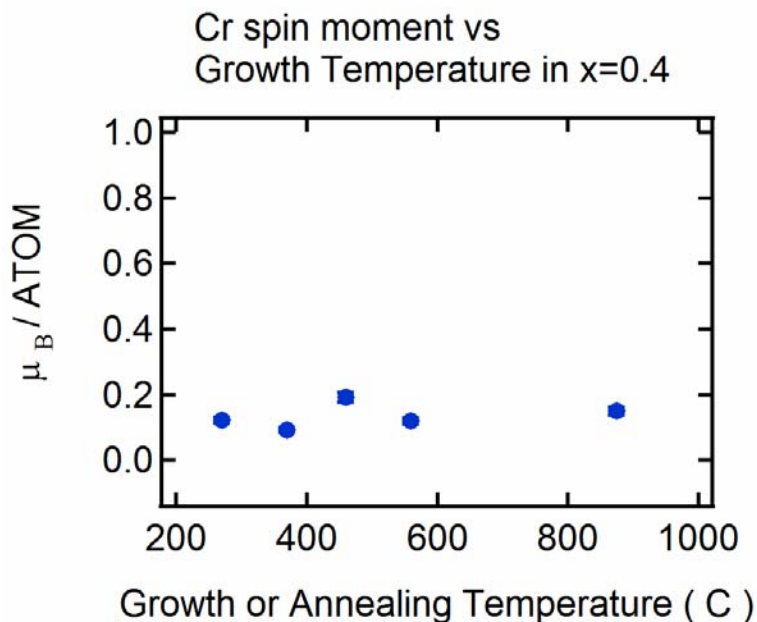
$$m_{\text{orb}}(\text{Co}) \sim 0.1 \mu\text{B} / \text{atom}$$

L21 Theory from
Galanakis, private communication

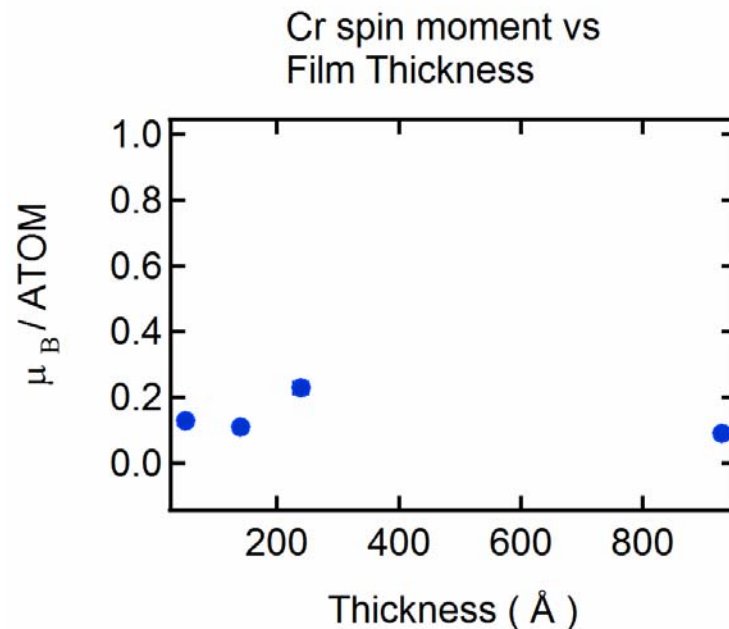
Cr Spin Moments in $\text{Co}_2\text{Cr}_{0.6}\text{Fe}_{0.4}\text{Al}$

The Cr spin moment remains small across samples grown at different temperatures and of different thicknesses

vs. Temperature



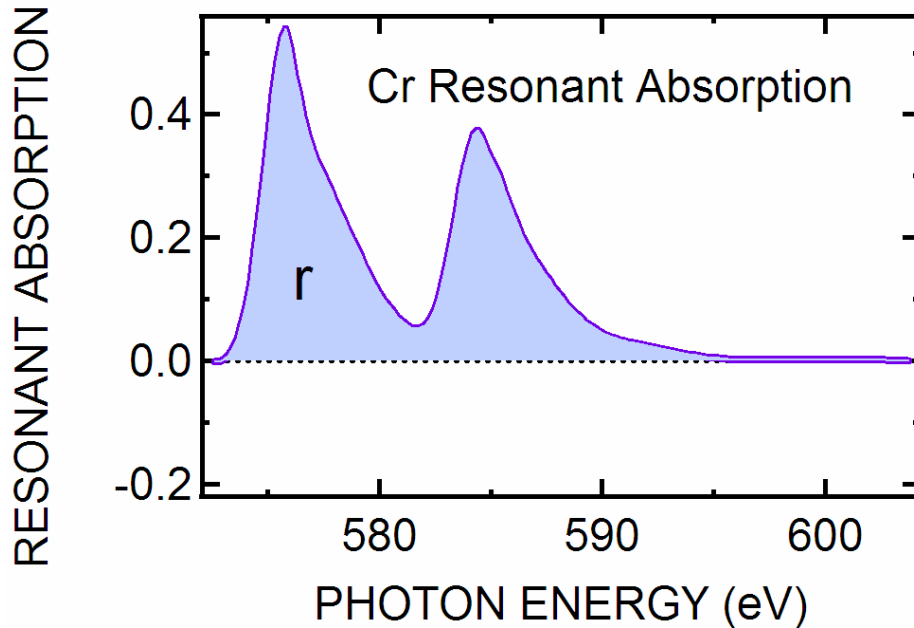
vs. Film Thickness



Estimation of number of d holes

- Can estimate number N_{3d} from absorption spectra

- $N_{3d} = r * C$



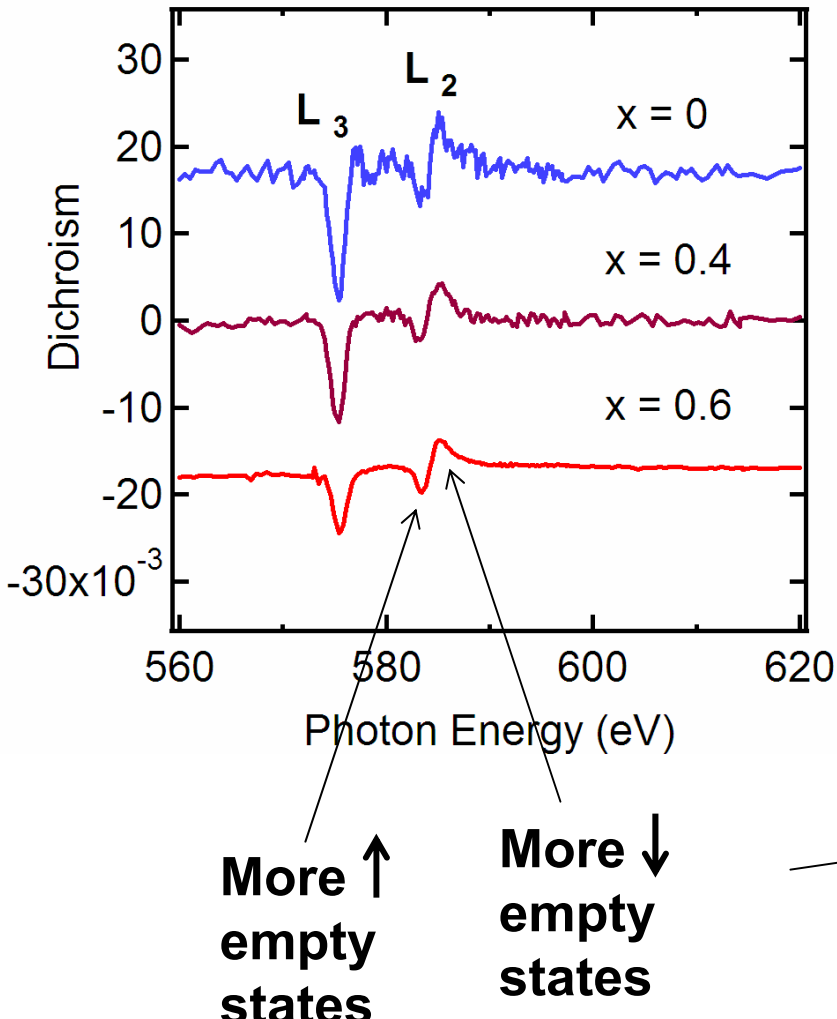
Average of N_{3d} for
 $x = 0.4$ samples

	Exp. Avg. $x=0.4$	Theory $x=0.375$
Fe	3.4	3.5
Co	2.6	2.3
Cr	1.8	5.4

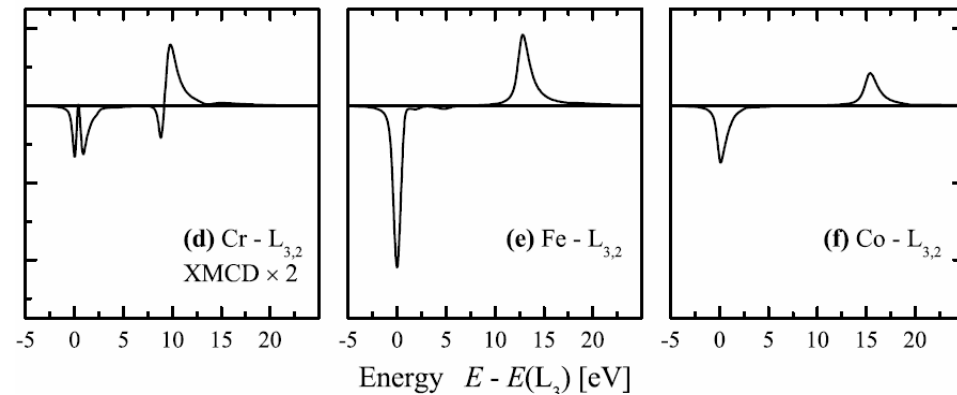
Theory values from Antonov et.
al, Phys. Rev. B 72, 054441
(2005)

Change of sign in Cr dichroism spectra

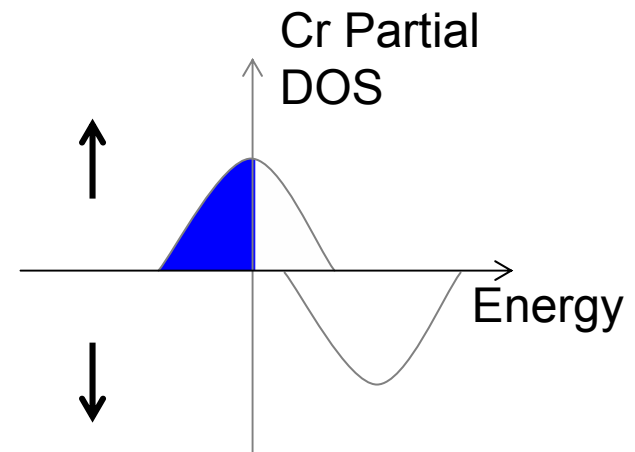
Cr dichroism spectra
for different compositions



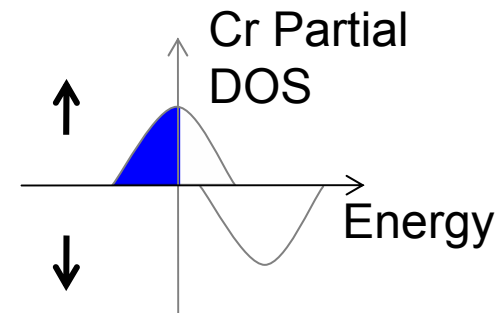
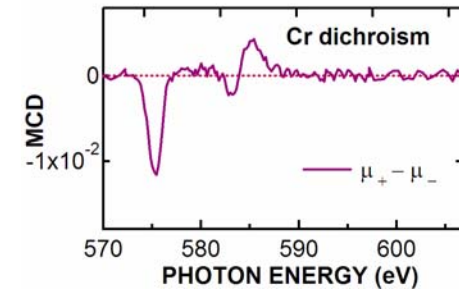
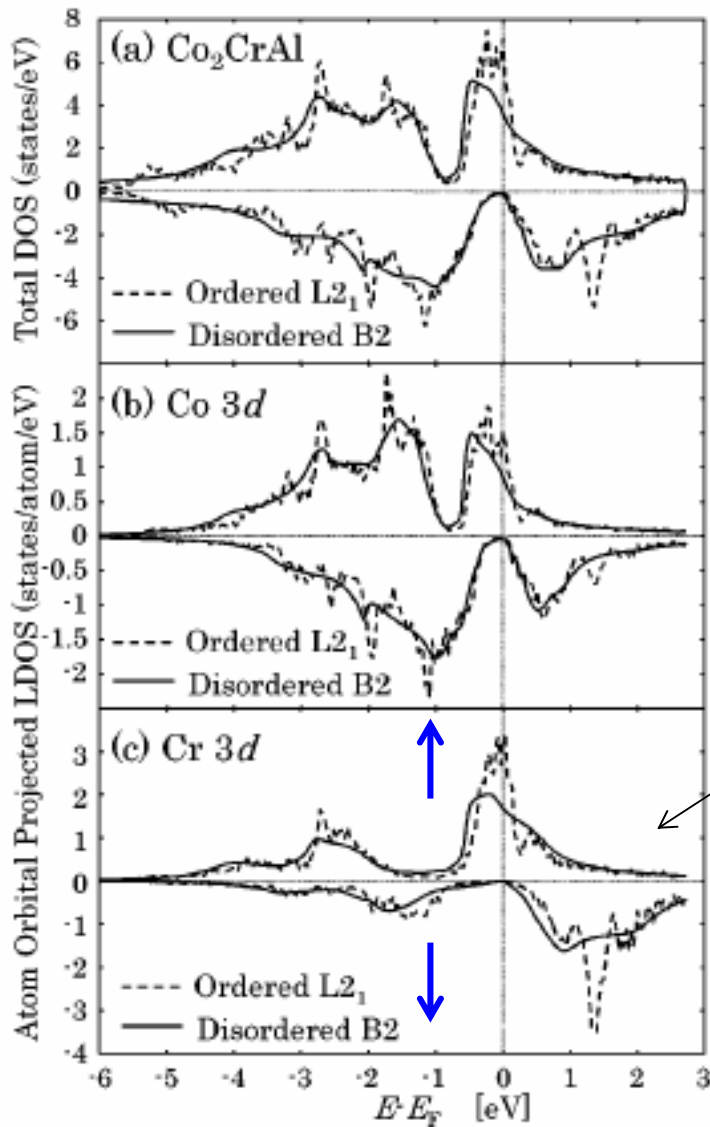
Calculated dichroism spectra for $x=0.4$



Wurmehl et. al, J. Phys. D 39, 803 (2006)



Cr dichroism spectra

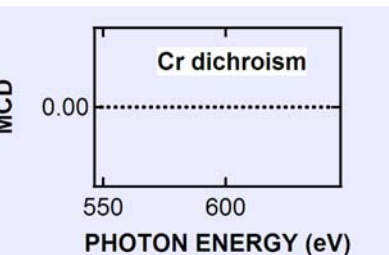
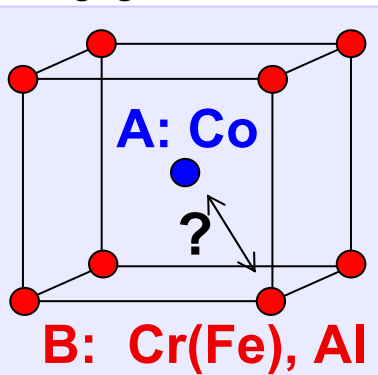


- A large Cr PDOS can be seen above Fermi level, even for B2 structure
- Large shift for Cr and not for Co
- Associated with a large Cr moment

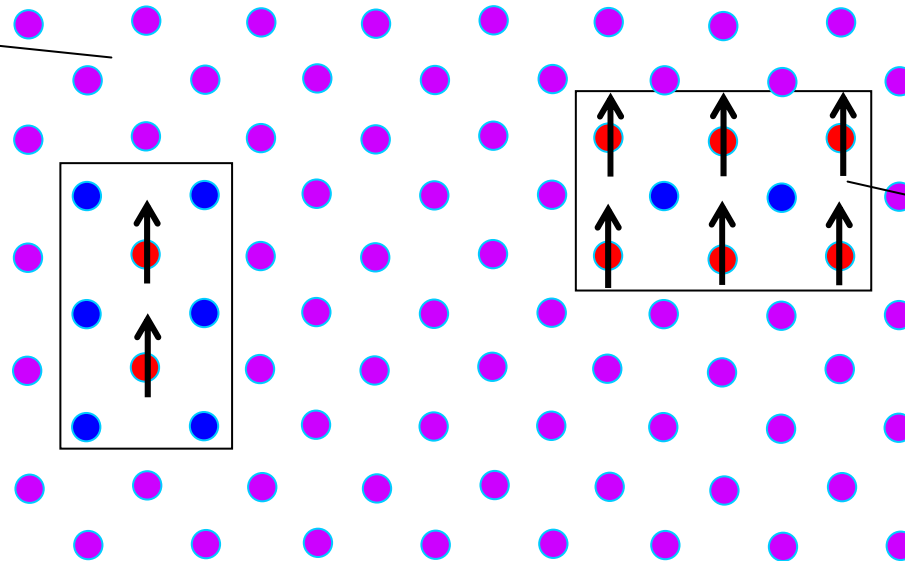
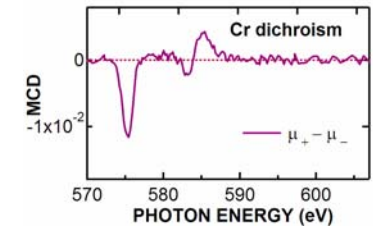
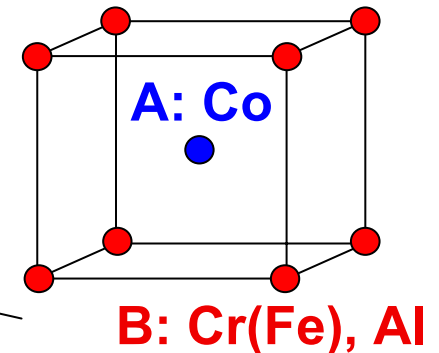
Two Types of Regions

- Low $N_{3d}(\text{Cr})$ from $N_{3d} = r * C$
- Cr dichroism line shape follows B2 DOS
- Fe and Co are less sensitive to disorder

Disordered B2:
Negligible Cr moment



Ordered B2:
Cr moment

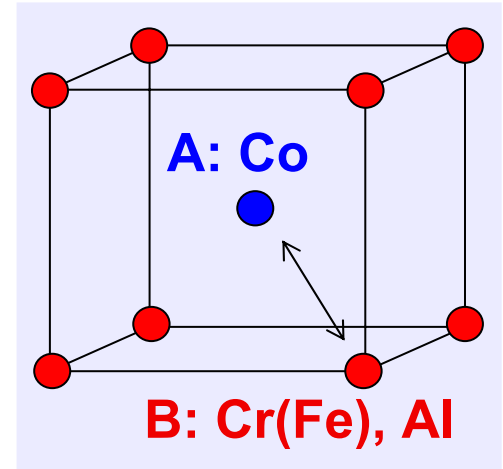


Outline

- I. Description of Half Metals and Reasons For Studying $\text{Co}_2\text{Cr}_{1-x}\text{Fe}_x\text{Al}$
- II. Epitaxial Growth and Basic Characterization of $\text{Co}_2\text{Cr}_{1-x}\text{Fe}_x\text{Al}$
- III. Incorporation of Epitaxial $\text{Co}_2\text{Cr}_{1-x}\text{Fe}_x\text{Al}$ into Superlattices and Spin Valves
- IV. Electronic and Magnetic Properties of Single-Layer Epitaxial Films
 - A. Measurement of the Spin Polarization
 - B. Study of the Elemental Magnetic Moments
 - C. Quantifying Atomic Disorder
- VI. Conclusions

Atomic Disorder in Heusler Alloys

- Atomic disorder proposed in general for Heusler alloys
Orgassa et. al, J. Appl. Phys. 87, 5870 (2000)
Picozzi et. al, Phys. Rev. B 69, 094423 (2004)
Miura et. al, Phys. Rev. B 69, 144413 (2004)
- Only experimental study in Co_2MnGe → nonstoichiometry
Ravel et. al, APL 81, 2812 (2002)
- Results from this work could shed light on related materials as well



Atomic Disorder in $\text{Co}_2\text{Cr}_{1-x}\text{Fe}_x\text{Al}$ With Anomalous X-ray Diffraction

- Studied (001) reflection \rightarrow sensitive to A-B disorder

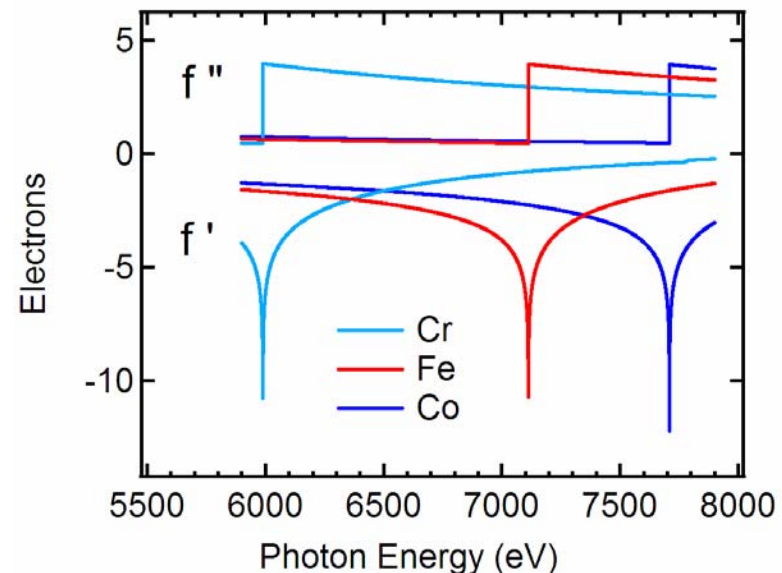
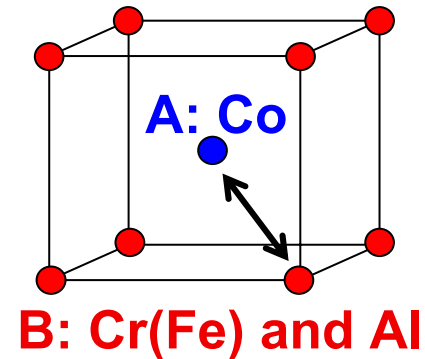
$$|F_{001}| = |f_A - f_B|$$

- f_{Cr} , f_{Fe} , and f_{Co} nearly identical at Cu $K\alpha$ energy

- Work near absorption edges \rightarrow

- In general

$$f(q, E) = f_o(q) + f'(E) + i \cdot f''(E)$$



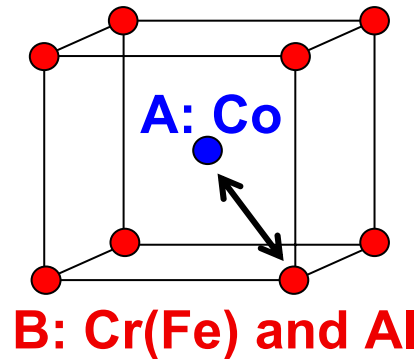
Modeling Atomic Disorder in $\text{Co}_2\text{Cr}_{1-x}\text{Fe}_x\text{Al}$

- Model disorder with two parameters:

d_0 : Co on Site B

d_1 : Cr(Fe) on Site A

→ $F_{001}(d_0, d_1)$ and F_{002}



$$I_{hkl}(q, E) = I_o \left| F_{hkl}(q, E) \right|^2 \frac{1}{E^3 \sin 2\theta} \frac{1 - e^{\frac{-\mu(E)t}{\sin \theta}}}{2\mu(E)} e^{-2Mq^2}$$

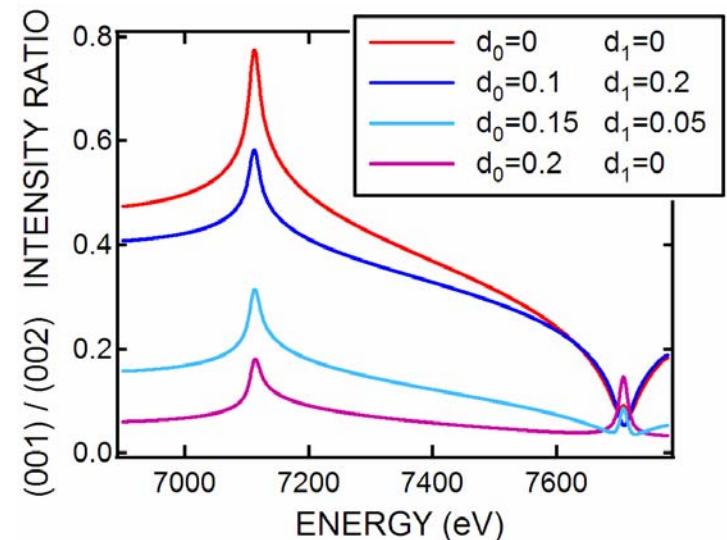
Structure Factor

Lorentz-Polarization

Absorption

Debye Waller

Convolute with a gaussian

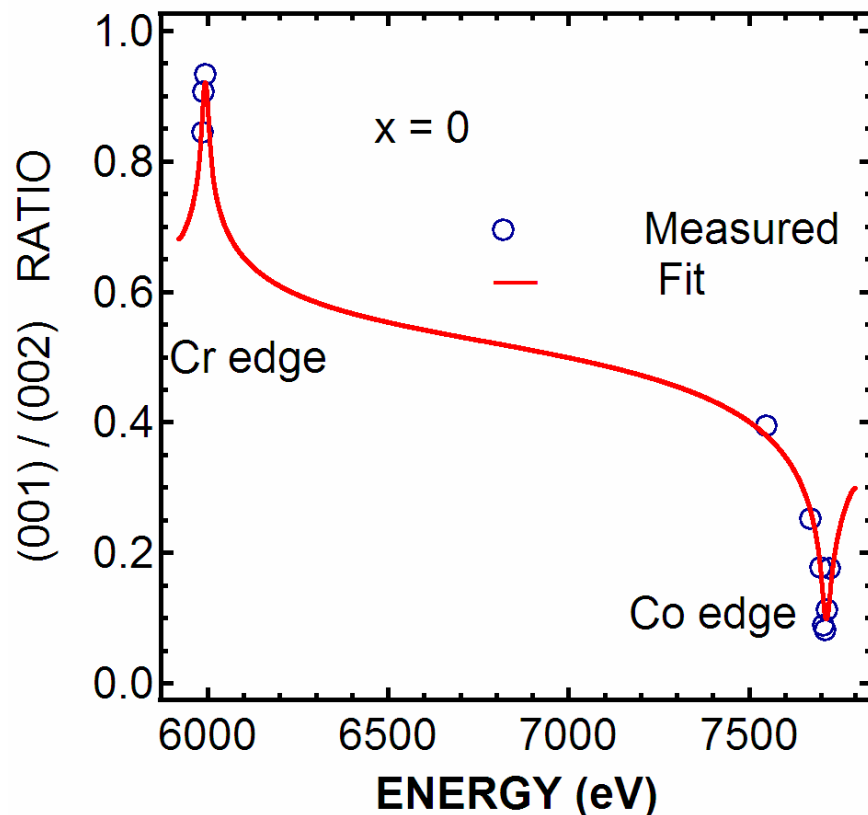


Anomalous Diffraction Data and Fits

For $x = 0$

3 pts at Cr edge

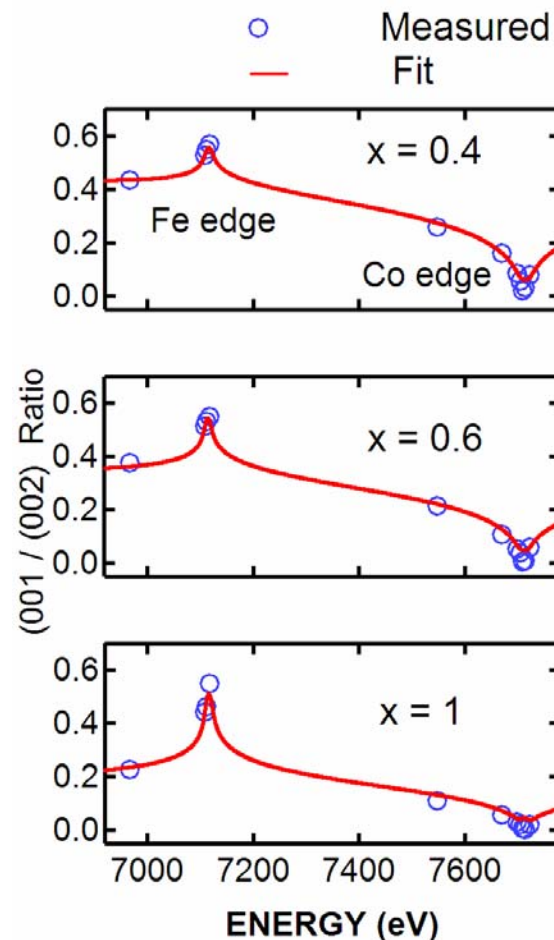
8 pts at Co edge



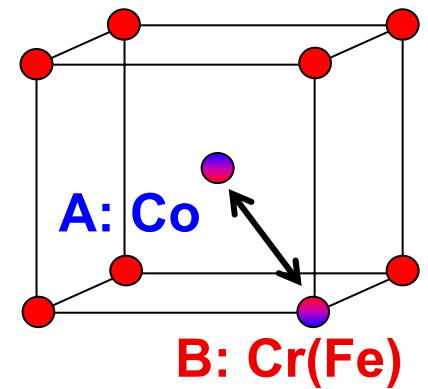
For $x = 0.4, 0.6, 1$

4 pts at Fe edge

8 pts at Co edge



Atomic Disorder Results



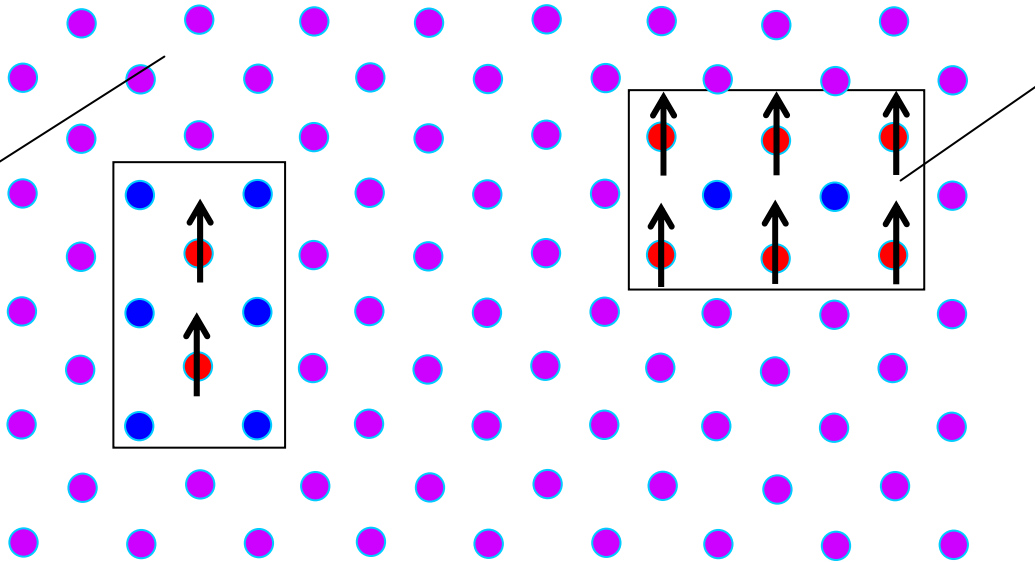
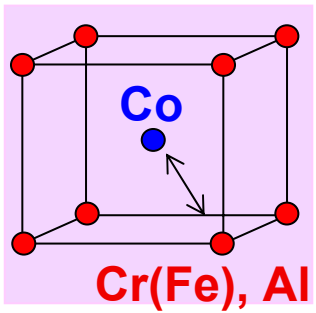
Average disorder over entire sample

Sample	d0	d1	Site A			Site B		
			Co	Cr(Fe)	Al	Co	Cr(Fe)	Al
$\text{Co}_{1.12}\text{Cr}_{0.39}\text{Al}_{0.49}$ ($x=0$)	0.21 ± 0.01	0.24 ± 0.02	91	9	0	21	30	49
$\text{Co}_{1.03}\text{Cr}_{0.32}\text{Fe}_{0.2}\text{Al}_{0.45}$ ($x=0.4$)	0.11 ± 0.01	0.15 ± 0.04	92	8	0	11	44	45
$\text{Co}_{0.99}\text{Cr}_{0.21}\text{Fe}_{0.3}\text{Al}_{0.5}$ ($x=0.6$)	0.05 ± 0.01	0.13 ± 0.04	94	6	0	5	45	50
$\text{Co}_{1.04}\text{Fe}_{0.5}\text{Al}_{0.46}$ ($x=1$)	0.09 ± 0.01	0.06 ± 0.05	95	3	2	9	47	44
B2 Structure								
$\text{Co}_2\text{Cr}_{0.5(1-x)}\text{Fe}_{0.5(x)}\text{Al}_{0.5}$	0	0	100	0	0	0	50	50

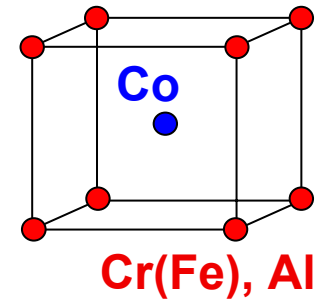
Co Anti-Site Disorder

- Two Regions
 - 1) Ordered B2: no Co disorder
 - 2) Disorderd B2: Co anti-site disorder ~ 10% for low x films
- Explains
 - High resistivity in the Cr containing alloys
 - Reduction of magnetization
 - Reduced spin polarization

Co anti-site
disorder ~ 10%



Ordered B2



Conclusions

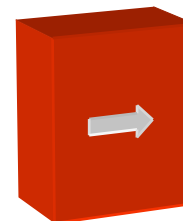
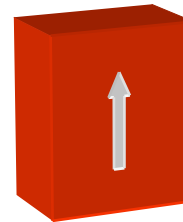
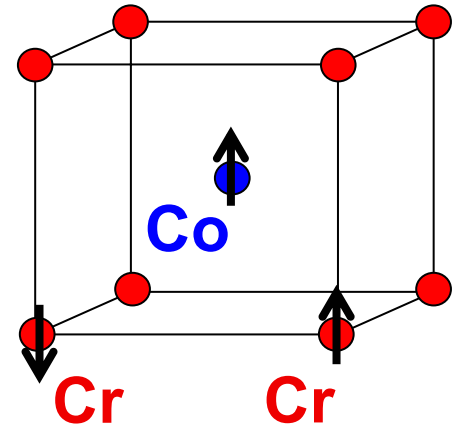
- Grown for the first time epitaxial thin films and superlattices of $\text{Co}_2\text{Cr}_{1-x}\text{Fe}_x\text{Al}$
- Demonstrated for the first time a large giant magnetoresistance, up to 7% at room T, in a predicted half metal
- Measured a spin polarization of 50%
- Modified sum rules for x-ray dichroism to measure a reduced average Cr spin moment of $0.2 \mu_B \rightarrow$ inferred regions with magnetic Cr and non-magnetic Cr
- Measured anti-site Co disorder $\sim 10\%$ for low x
- Future efforts to resolve disorder could lead to a highly spin polarized and even more promising material

Acknowledgements

- Jo Stohr at SSRL
- Michael Toney at SSRL
- Raghava Panguluri and Boris Nadgorny at Wayne State University
- Arturas Vailionis
- Hertz Foundation

Magnetic Linear Dichroism

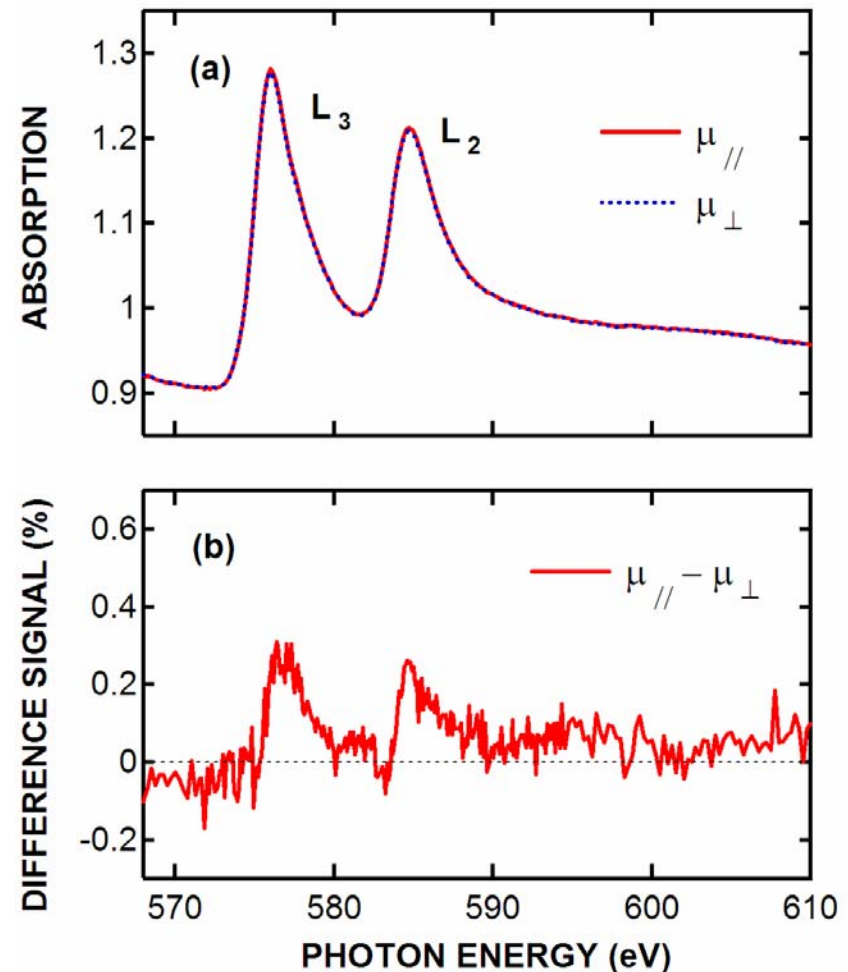
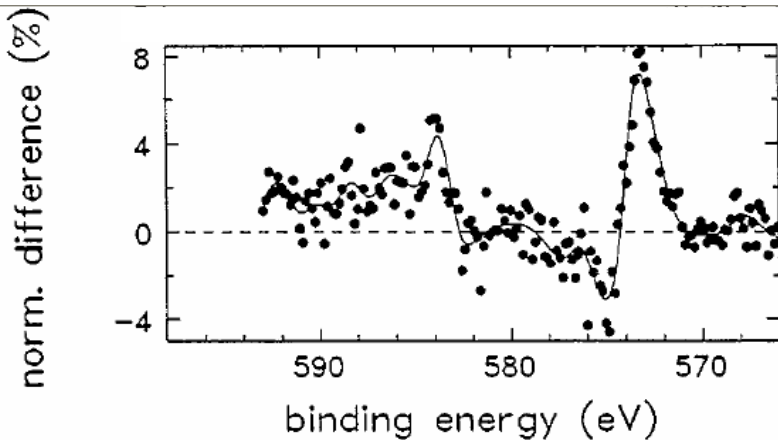
- Magnetic circular dichroism measures $\langle M \rangle$ along \vec{k}
- Magnetic linear dichroism measures $\langle M^2 \rangle$



Antiferromagnetic Coupling Among Cr?

Cr Difference Signal
in $\text{Co}_2\text{Cr}_{0.6}\text{Fe}_{0.4}\text{Al} \rightarrow$ No AF coupling

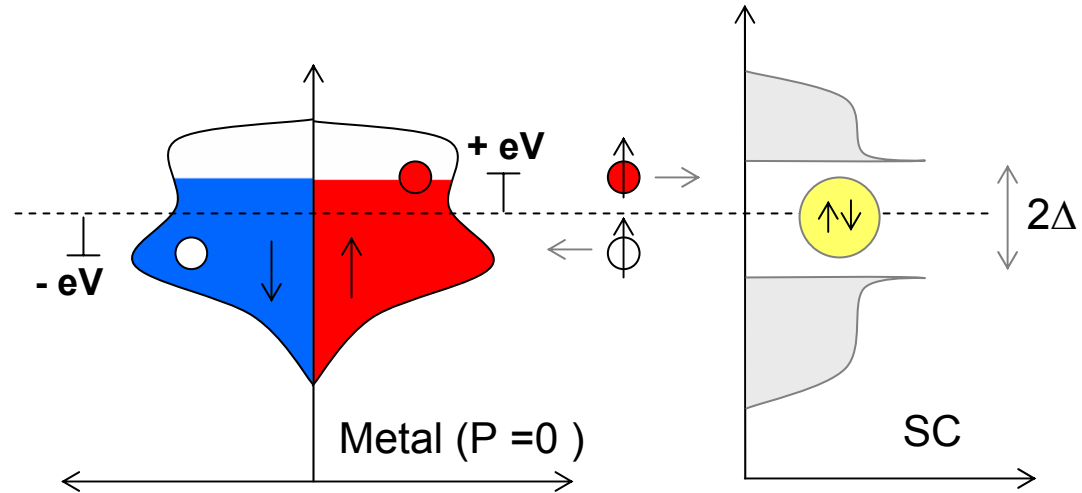
Reference:
Cr Difference Signal for AF-coupled
Cr on Fe [Knabben et. al, J. Of Elec.
Spec. and Rel. Phenom. 86, 201 (1997)]



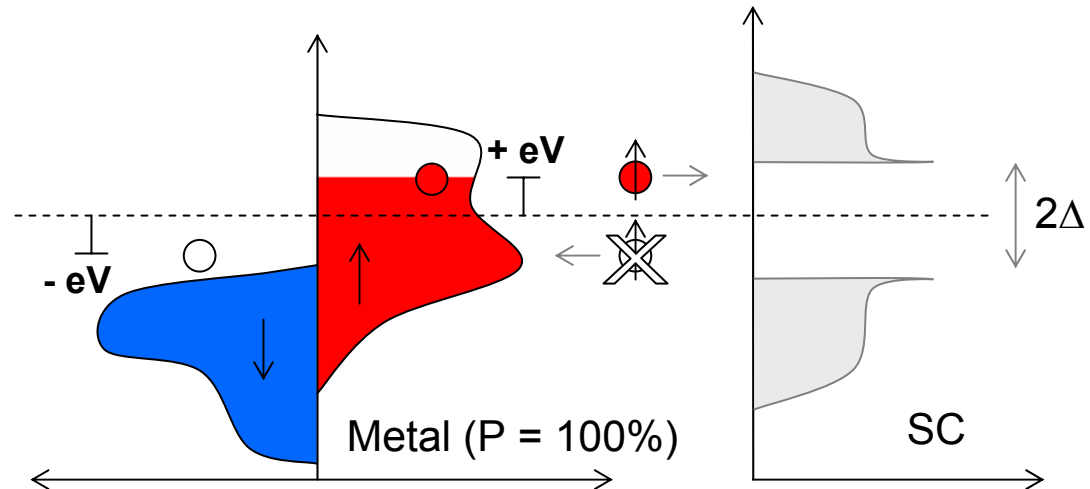
Schematic of PCAR Spectroscopy

- Compared to the case of $eV > \Delta$

Normal Metal, $eV < \Delta$
Conductance is doubled

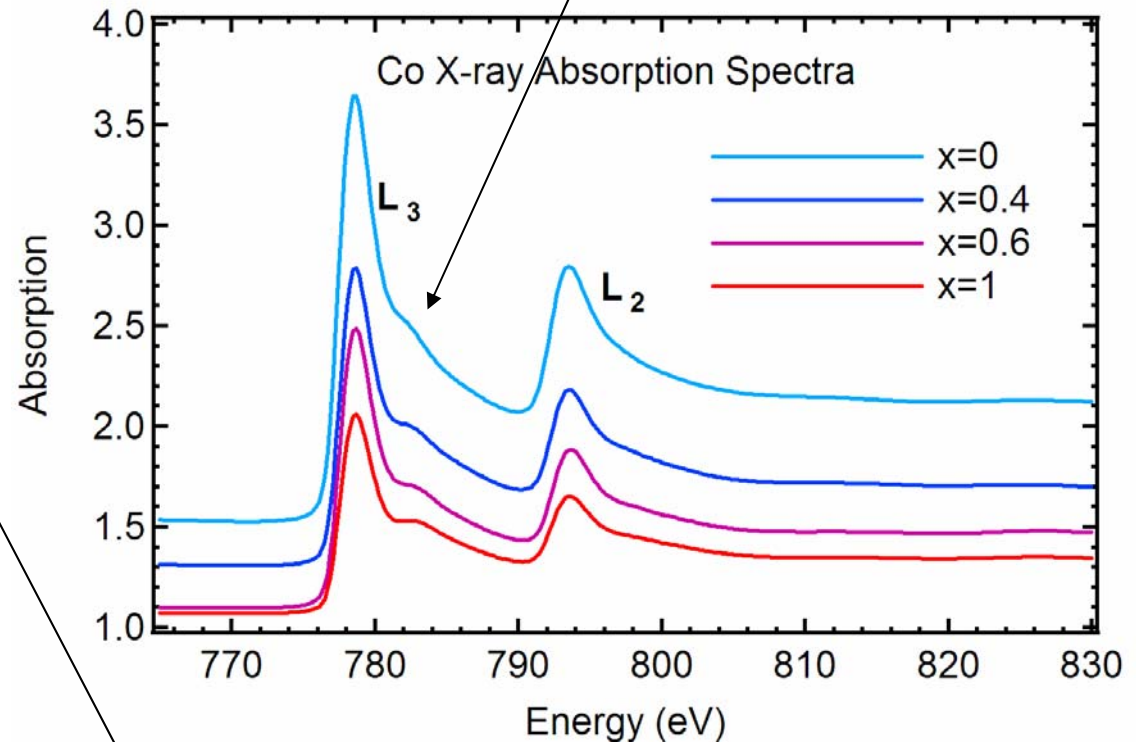
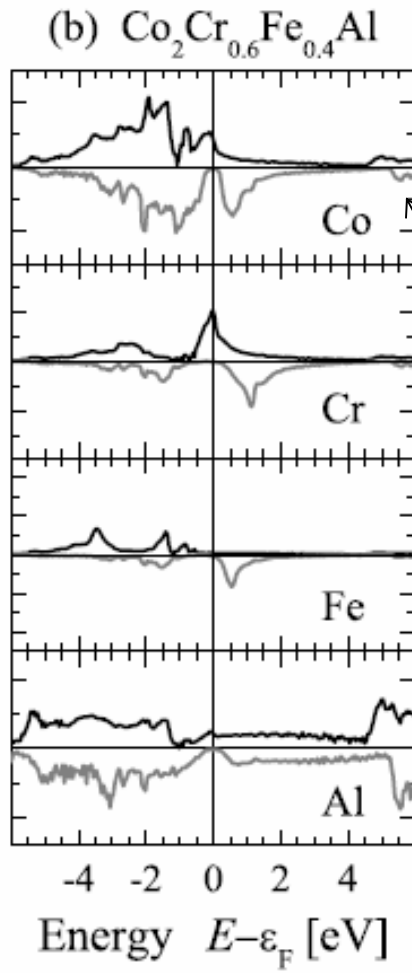


Half Metal, $eV < \Delta$
Conductance is zero



Origin of shoulder on Co L_3 edge

Shoulder not seen in pure Co

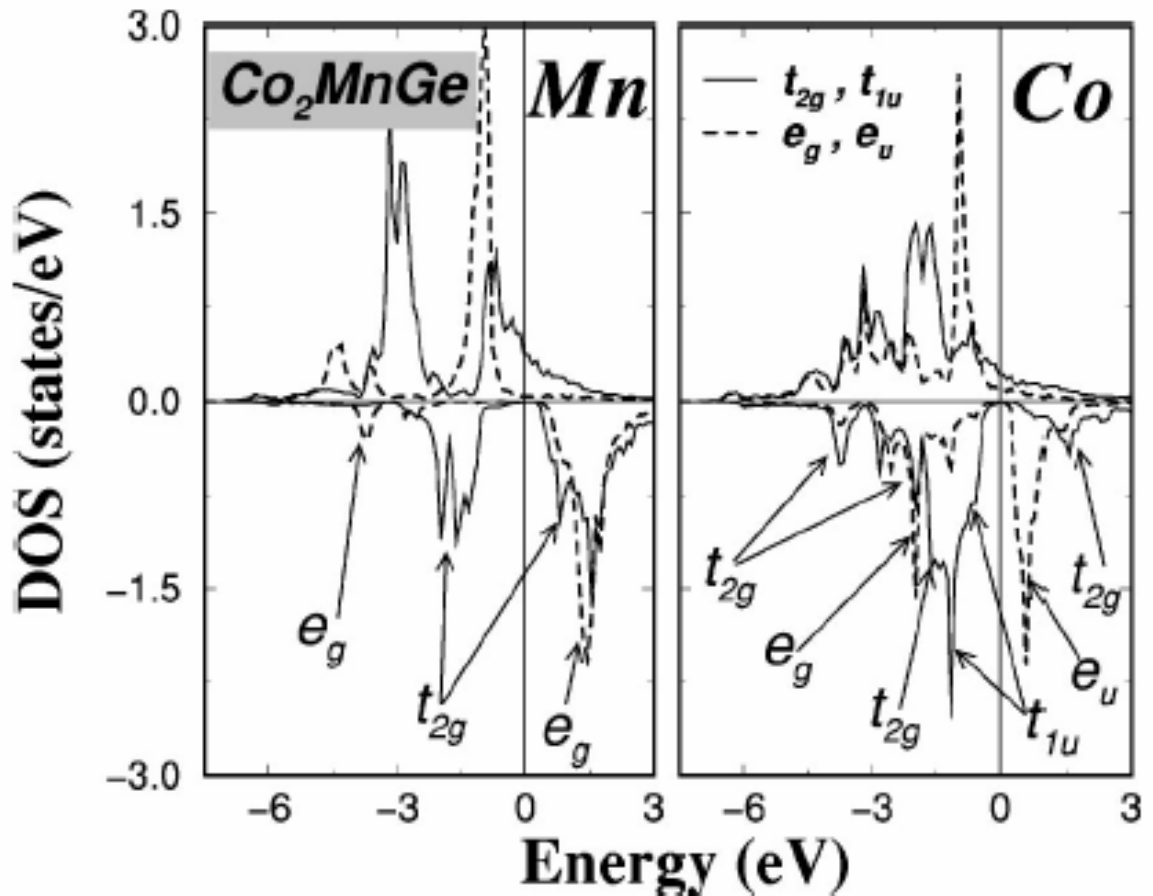


Origin of shoulder;
indicates Co-Al
hybridization → doesn't
show up in dichroism

Effects of B2 Disorder on Gap?

Galanakis et. al proposed that in Co_2MnGe the states near the Fermi level were nonbonding Co states

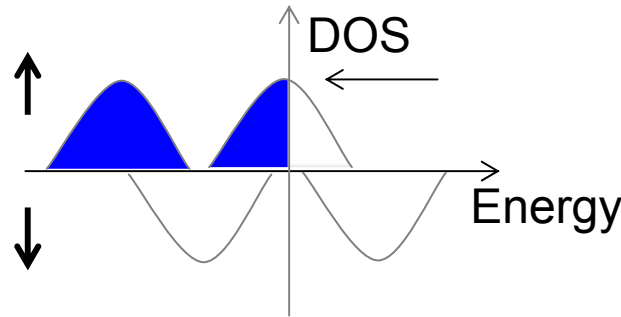
These states do not hybridize due to their unique octahedral symmetry



Galanakis et. al, Phys. Rev. B 66, 174429 (2002)

Elemental Spin Magnetic Moments From DOS Calculations

Effect of adding Fe $\rightarrow M_s = 3 + 2x$ for $\text{Co}_2\text{Cr}_{1-x}\text{Fe}_x\text{Al}$ in $L2_1$



- Co spin moment increases from ~ 0.8 to $1.22 \mu_B$
- Fe moment $\sim 2.8 \mu_B$
- Cr moment $\sim 1.5-1.6 \mu_B$

Galanakis, private communication

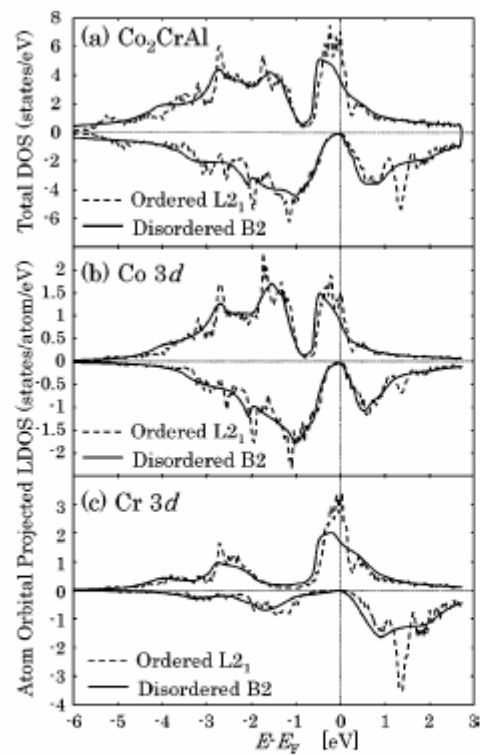


FIG. 2. Density of states of the majority-spin (positive) and the minority-spin (negative) components of Co_2CrAl with the ordered $L2_1$ structure (solid line) and with the disordered $B2$ structure (broken line). (a) Total DOS of Co_2CrAl . (b) Atom orbital projected local DOS for Co. (c) Atom orbital projected local DOS for Cr. The vertical dotted lines indicate the position of the Fermi level (E_F).

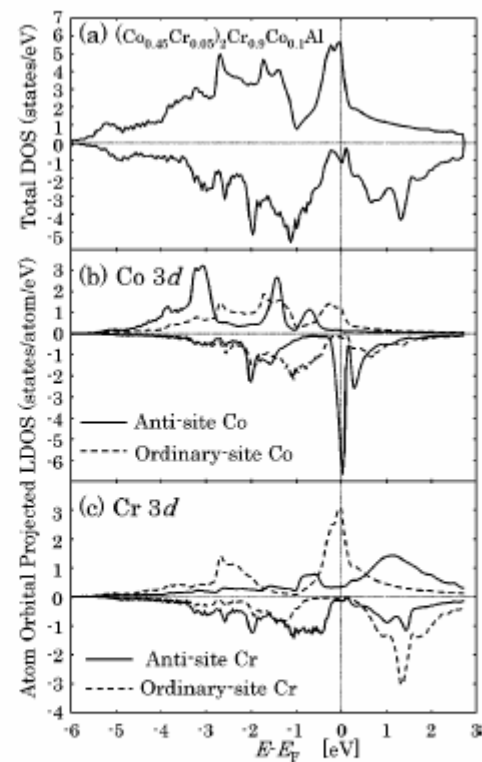
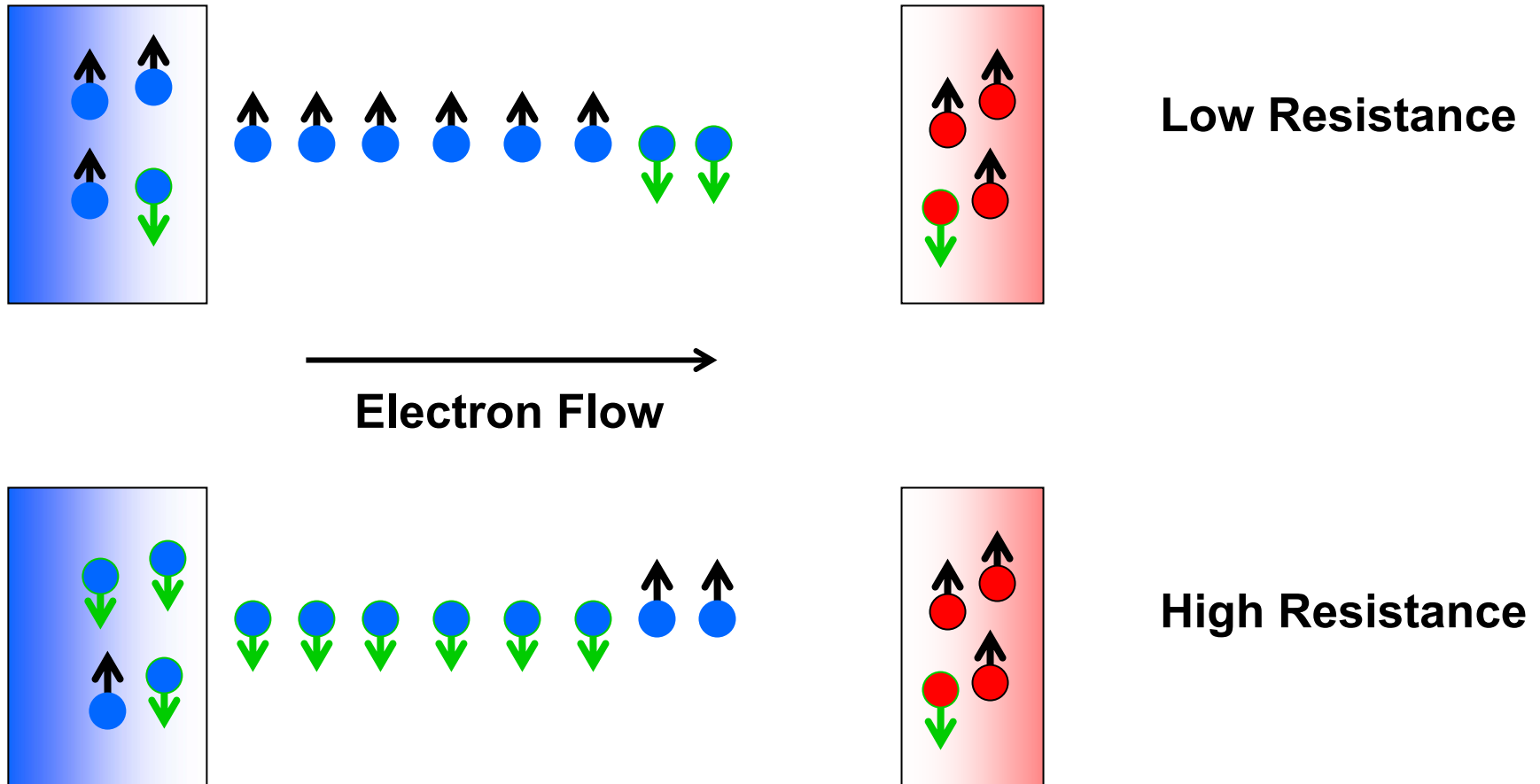


FIG. 3. Density of states of Co_2CrAl with the Co-Cr type disorder (the disorder level of 0.1). (a) Total DOS. (b) Atom orbital projected local DOS for Co. (c) Atom orbital projected local DOS for Cr.

Basis for Applications of Half Metals

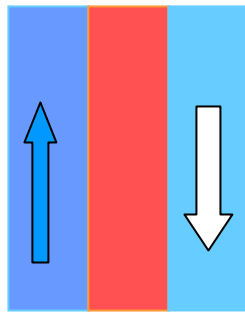


Applications:

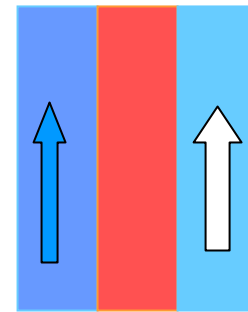
Spin Transfer Magnetization Switching

Two ferromagnets separated by a nonmagnetic metal

Current
→



$t=0$



$t=\tau$

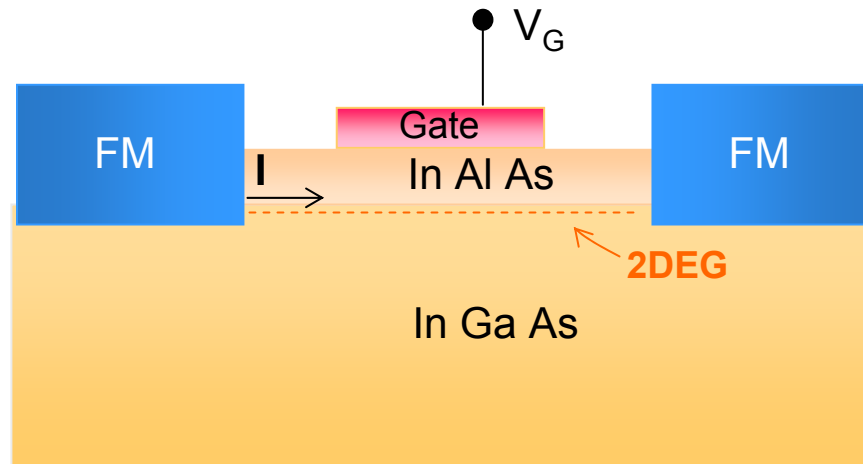
Exchange interaction between injected spins and atomic moments can switch atomic moments

J. C. Slonczewski, J. Magn. Magn. Mater. **159**, L1 (1996)

Applications:

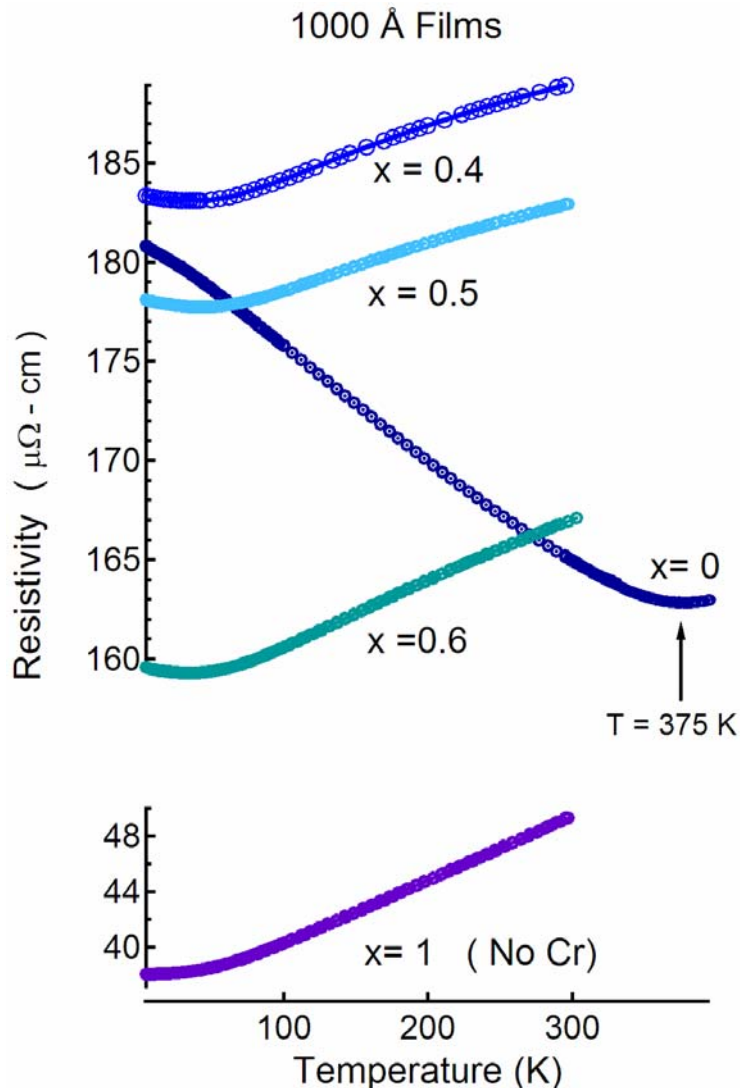
Spin Injection Into Semiconductors

- Spin Transistors, Datta and Das, APL 56, 665 (1990)



Change $V_G \rightarrow$ Current "ON" and "OFF"

Co₂Cr_{1-x}Fe_xAl Resistivity



For $x < 1$

- high resistivity
- upturn at low temperature indicates short mean free path
- Curie temperature for $x=0$ reflected in resistivity

For $x = 1$

- Resembles a conventional metallic ferromagnet